International Journal of Precision Engineering and Manufacturing-Green Technology
https://doi.org/10.1007/s40684-025-00731-2

Online ISSN 2198-0810
Print ISSN 2288-6206

REGULAR PAPER

Comparative Life Cycle Assessment of Different Pre-treatment Scenarios for Diamond Coating Deposition on WC–Co Through HF-CVD

Emanuele Mingione[1] · Mattia Gianvincenzi[1] · Marco Marconi[1] · Gianluca Rubino[1]

Received: 28 November 2024 / Revised: 27 February 2025 / Accepted: 9 March 2025

Abstract

This study compares the environmental impact and durability of diamond-coated WC–Co substrates produced via the Hot Filament Chemical Vapor Deposition (HF-CVD) process with different pre-treatment and deposition conditions. Diamond coatings on WC–Co substrates offer significant wear resistance, making them ideal for various industrial applications. However, the process faces challenges due to residual stresses from thermal expansion differences and chemical reactions between cobalt binders and carbon-rich gases, which may cause poorly adherent coatings. Various pre-treatment techniques, such as chemical etching and laser methods, are essential to improve coating adhesion and prevent graphite formation through the selective removal of the binder. This study conducts a comparative Life Cycle Assessment analysis of two industrial pre-treatment methods, Murakami's chemical etching and diode laser treatment, and investigates the environmental impact of using two assistant gases (Nitrogen and Argon) and two Methane/Hydrogen ratios (1% and 2%) in HF-CVD. To overcome the gaps present in previous studies, wear and service life were considered across the six scenarios by defining the wear ratio, obtaining more accurate results in terms of environmental impact. From the ReCiPe midpoint, endpoint and GWP analysis emerges that Chemical Etching with 2% CH_4/H_2 is the least impactful scenario for the overall deposition process, while laser pretreatments have better ReCiPe indicators if is considered only the pre-treatment phase. The results aim to guide manufacturers in optimizing pre-treatment processes and deposition conditions for enhanced sustainability, taking into account both technical and environmental factors.

Keywords HF-CVD · Diamond coating · LCA · WC–Co · Chemical etching · Fibre laser

1 Introduction

Coating hard metals with ultra-hard materials such as diamond is highly desirable, as it significantly extends their wear life beyond standard performance levels [1]. Co-cemented tungsten carbides (WC–Co), are a class of hard metals commonly used in the production of cutting tools, sliding bearings, drawing dies, and a wide range of wear-resistant components [2]. Diamond deposition on WC–Co substrates is particularly attractive for applications requiring high wear resistance, in particular, the combination of the carbide's hardness and the binder's toughness results in exceptional mechanical properties, which can be further improved with diamond coatings [3, 4].

Depositing diamond coatings onto Co-cemented tungsten carbide encounters several challenges due to mechanical, chemical, and thermal factors [5–7]. The disparity in the coefficients of thermal expansion between diamond and WC–Co, stemming from the Co-based binder in the WC–Co substrate, causes significant residual stresses in the coating. Different methods can be used to deposit diamond coatings on WC–Co substrates, such as Chemical Vapor Deposition (CVD) [8, 9], Physical Vapor Deposition (PVD) [10], and Electrochemical Deposition [11]. Among the techniques which involves a CVD process, Hot Filament CVD (HF-CVD) is the most industrial relevant one compared to the Microwave Plasma Assisted CVD (MP-CVD) and Direct Current Plasma CVD (DC-PCVD) due to the lower costs compared to the other ones and the ability to coat large areas uniformly [12, 13]. In this method, a hot tungsten filament is used to decompose a carbon-containing gas (usually CH_4) in

✉ Emanuele Mingione
emanuele.mingione@unitus.it

[1] Department of Economics, Engineering, Society and Business Organization, Università degli Studi della Tuscia, Largo dell'Università, 01100 Viterbo, Italy

Published online: 14 April 2025

the presence of hydrogen. The carbon atoms then nucleate and grow as diamond crystals on the substrate. Due to the high temperatures achieved during the process, the alloying cobalt present in the substrate can react with the carbon-rich gas phase, quickly becoming saturated with carbon [14], and favoring the formation of an intermediate graphite layer, which supports poorly adherent thin diamond layers [15].

For these reasons, an effective surface pre-treatment is crucial for removing the Co at the interface from the WC–Co substrate before diamond film deposition and preparing the surface morphologically to ensure a durable and adherent coating. The pre-treatment process can be executed using several methods, such as chemical etching [16, 17], usage of interlayers [18, 19] and thermochemical treatments [20, 21].

The first technique entails an etching process to remove Co from the surface by using concentrated acids, such as nitric or hydrochloric ones, generally for durations of 10–15 min. Among these methods, the most known one is the Murakami's treatment [20], which involves a multi-step process. In the first step, the Co-cemented tungsten carbides are etched using a solution of potassium iron cyanide and potassium hydroxide in water (10 g KOH + 10 g $K_3[Fe(CN)_6]$ + 100 ml water) up to approximately 30 min. The second step uses Caro's acid, which is a mixture of sulfuric acid and hydrogen peroxide (96 wt% H_2SO_4 + 40% w/v H_2O_2), to chemically etch the substrate for a very short duration. This technique effectively removes Co while simultaneously corrugating the WC–Co substrate, in order to improve the adhesion of the deposited film [19]. Despite the effectiveness and the high speed of the treatment, the usage and disposal of the aforementioned acids potentially represent an environmental issue for this kind of processes [22, 23].

The second methodology consists in the applications of interlayers which acts as a diffusive barrier for the Co and avoids the contact with the carbon, preventing the formation of sp2 hybridised graphite. The technique of applying interlayers, such as amorphous carbon, metallic Cr, Ti, Ta, and ceramics like CrN, TiC, TiN, SiC, and Si_3N_4 between Co-cemented tungsten carbides and diamond coatings, is well-known in scientific literature, and has different advantages [24]. The first benefit occurs because surface cobalt is not removed and there is no weakening of the interface caused by removal of the binder. In addition, the presence of an interlayer with an intermediate thermal expansion coefficient between the coating and substrate reduces the internal residual stresses that are created during cooling after deposition. However, such process is not used in the industrial practice due to significant time, difficulties of automating the process and the high cost of materials used [25].

The third option includes thermochemical treatments, which are industrially feasible for pre-treating Co-cemented tungsten carbides [20, 21]. Among these ones, laser treatments, such as pulsed laser and continuous diode laser techniques, are particularly notable. Pulsed laser sources modify the surface by repetitive pulsed excimer laser irradiation ($\lambda = 250$–300 nm, $\tau = 20$–25 ns) [24–26]. The selective removal of Co happens due to the different melting and boiling points of Co (1768 K and 3200 K) and WC (3143 K and 6273 K), as well as their different absorption coefficients. When the laser beam irradiates the WC–Co composite, WC absorbs more energy and retains it, leading to the local melting and vaporization of the surrounding Co [20]. This process, compared to the other two previously analyzed, allows the removal of surface cobalt without using toxic substances that are difficult to dispose of, and with reduced treatment time and cost compared to the application of interlayers.

In the current European environmental and raw materials policies is emphasized the importance of sustainability and circularity to address pressing ecological and resource challenges.

In scientific literature, LCA has been widely used to evaluate the sustainability of emerging technologies across various industrial sectors [26]. Recent studies have demonstrated that its application can provide valuable insights for developing lower-impact processes and supporting decision-making in adopting new technologies at an industrial level. For instance, Venettacci et al. [27] applied LCA to compare the environmental impact of surface finishing processes in the aerospace sector, showing a 45% reduction in overall impacts when adopting innovative technologies compared to traditional methods. Similarly, Müller-Carneiro et al. [28] emphasized the importance of Ex-Ante LCA for assessing novel technologies in the research and development phase, addressing challenges related to data uncertainty and large-scale production modeling. Lastly, Fernández-González et al. [29] highlighted how LCA tools are crucial in developing emerging decarbonization technologies, contributing to the transition toward low-carbon production processes. These studies underscore the central role of LCA in evaluating the sustainability of technological innovations, providing a methodological reference for studies such as the present one.

Following a review of the scientific literature, it is evident that studies done on the diamond deposition on WC–Co substrates through HF-CVD emphasize the mechanical performance of the coating, enhancing the material usage for machining tools and components commonly used in the mechanical industry [30]. Conversely, researches on the environmental impacts of manufacturing WC–Co are very limited, or include different simplifications, such as lack of relevant inventory data [31], consideration of few impact categories, neglection of some life cycle phases as disposal of substances used for the treatments or even lack in considering the duration of the service life of coatings realized with alternative techniques.

Wilfong et. al. [32] measured the environmental effects of applying a thin diamond film to cutting tools, in particular for the conditions evaluated, the primary deposition process was found to have a carbon footprint of 6.6 $kgCO_2eq$, and the etching process was found to be responsible for 96.8 $kgCO_2eq$. However, the Life Cycle Assessment (LCA) study was done without considering other impact categories (e.g. those ones included in the of ReCiPe methodology) and without any comparison between different form of pretreatments and how they affects the tool life due to the different wear resistance of the WC–Co deposited film.

Marconi et al. [33] investigated the environmental and economic sustainability of two different substrate pre-treatment processes i.e. the chemical etching process, and high-power continuous wave diode laser method. The main results obtained from the LCA analysis showed that for most of the ReCiPe impact categories, the environmental impact of laser treatment is greater than that of the chemical process (+38% in case of Climate Change, +45% in case of ReCiPe endpoint Single score), attributed to due to the high energy consumption of the laser. Conversely, the cost estimation highlighted relevant savings for the laser process (about −98%), due to higher cost of chemicals than for electricity. Despite the comprehensiveness of the indicators evaluated, this analysis aimed to only compare two alternative of a single pre-treatment process, while it was not considered how different Methane/Hydrogen ratios used during the HF-CVD process affect the wear experienced by the coated WC–Co, and consequently the service life of the diamond coated tools.

This work aims to overcome the aforementioned limitations by presenting a comprehensive LCA study of the overall HF-CVD process (i.e. pre-treatment, seeding, deposition process) for producing diamond coated WC–Co by considering the two most used industrial pretreatments, which are: (i) chemical etching based on Murakami and Caro acids, and (ii) diode laser. In addition, two different assistant gases (Nitrogen and Argon), and two different Methane/Hydrogen ratios (1% and 2%) have been considered to model the CVD deposition. These are essential features of the study because they allowed to experimentally evaluate the wear on the 6 different scenarios (see Sect. 2.2), and thus to define the duration of the service life of each sample in order to have a common base of comparison among the alternative scenarios. The consideration of different impact assessment methodologies, at both midpoint and endpoint levels, allows to have a global view on the environmental impacts and damages correlated with the pre-treatments and diamond coating depositions, as well as of the main causes. In a context where the sustainability of manufacturing processes is becoming of primary importance due to reasons of legislation compliance and competitiveness, the outcomes of this study could guide different industrial manufacturers (i.e. production of cutting tools, sliding bearings, drawing dies) and have a key role to guide in choosing the best option, jointly considering technical (i.e. wear) and environmental drivers. The reduction of LCA indicators, in particular those relating to air emissions, energy consumption, natural resource management, and waste disposal, is totally in line with the objectives of different industrially relevant regulations and standards (i.e. ISO 14001, REACH, and European voluntary declarations such as EMAS) [34].

The rest of the paper is organized as follows. Section 2 illustrates the materials used, the different process alternatives (scenarios) and the experimental tests performed to derive the wear of the different samples, used to model the service life within the life cycle models. Section 3 describes all the most relevant items of the first two LCA phases, goal and scope definition and life cycle inventory. Section 4 presents all the results obtained with the LCA study, together with a deep discussion and interpretation of them. Finally, Sect. 5 summarizes the most important conclusions of the present study and proposes some hints for future developments.

2 Material and Experimental Tests

2.1 Material and Process Scenarios

The specimens used for the experimentation were carbide (WC–Co) A09 plates with a square cross section of size 10 × 10 × 3 mm, as shown in Fig. 1. The samples were provided by "Fabbrica Italiana Leghe Metalliche Sinterizzate S.p.A.". In Table 1 were reported the WC–Co main properties declared by the manufacturer.

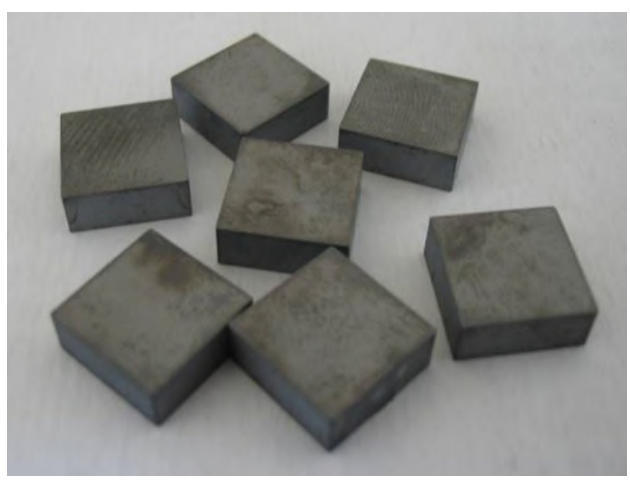

Fig. 1 WC–Co specimens used for the experiments

Table 1 Mechanical and electrical properties of the WC–Co used

Material properties	Values
wt% WC	94.2
wt% Co	5.8
Mean measure of the grains	0.7–0.8 µm
Density	14.8 g/cm^3
Elastic modulus	690 GPa
Transverse breaking load (ISO 3327)	2900 MPa
Hardness (vickers)	1743 HV10
Melting point	2800 °C
Electrical resistivity	22 µΩ/cm

Table 2 Main properties of the Rofin DL015 fibre laser system used

Laser system properties	Values
P_{max}	1500 W
Wavelenght	940 nm
Spot typology	Elliptical
Spot size	1.9 × 0.6 mm
Efficiency	30–50%
Assistant gas	Argon/nitrogen

As discussed in the Introduction, sample pretreatment is therefore a key step in the process of diamond deposition on WC–Co substrates, as its main purpose is to remove the binder phase from the surface of the samples used. In particular, in this study were compared the results in terms of performance obtained and sustainability of the overall processes of a standard chemical etching (Murakami + Caro's acid) and two different diode laser pretreatments, in which is used a different assistant gas (Argon/Nitrogen). The two different assistant gases were used because from previous works [20, 21] it was assessed that there are differences in terms of coating's adhesion after the HF-CVD deposition, which may affect the wear life of the coating.

The chemical etching was carried out by soaking the WC–Co samples in the Murakami's solution (10 g KOH + 10 g $K_3[Fe(CN)_6]$ + 100 ml water) for 30 min, and afterwards in Caro's acid, (3 mL 96 wt% H_2SO_4 + 88 mL 40% w/v H_2O_2), for 10 s.

Concerning the laser-based pre-treatments, instead, the fibre Laser system used for the experimental campaign is the Rofin DL 015, with its main properties shown in Table 2.

The choice of laser parameters used during pre-treatment was made taking into account optimizations that were carried out during previous experimental campaigns and analysis of the literature [14, 18, 32].

For all specimens treated with lasers, the power of the incident laser beam was fixed at 650 W and a processing speed of 1 mm/s was used [35]. The beam is moved back and forth along linear and parallel patterns to uniformly cover the entire substrate surface with an overlap of ~ 0.5–1.0 mm between two consecutive linear patterns. The treatment for each sample was repeated 3 times and lasted 30 min [21]. The choice of fixing a constant laser beam power, equal to 650 W, is dictated by the desire to achieve a pretreatment of the inserts, that allows for a consistent removal of the cobalt binder on the surface and an increase in surface roughness, preventing, at the same time, an excessive alteration of the microstructure of the tungsten carbide substrate. A beam power, of the diode laser, of 650 W is therefore the optimal power for the experimentation under consideration, as it results in only slight corrugation of the sample surface and removal of the cobalt binder in high percentages [36]. Higher powers would certainly have ensured advantages such as a greater removal of binder phase (Co) and increase in surface roughness which would help the successive nucleation of the diamond seeds. Despite the advantages, the increase in power leads to local melting and recrystallization of WC grains (with a consistent increase in surface grain size) and decarburization of the WC grains themselves, which potentially would have altered the surface microstructure of the substrate and thus compromised its mechanical properties [21, 36].

After each pretreatment, all samples were subjected to a seeding treatment, in an ultrasonic bath with a slurry of diamond particles (1/4 µm in diameter) and ethanol for 15 min, in order to implant nanometric diamond fragments, which act as growth centers during the HF-CVD process [20, 21, 37].

During the deposition phase the samples were placed in the CVD reactor on a Mo grid of 500 × 700 mm^2, within a distance of 50 mm between each one in both x and y direction of the grid, following a disposition of the specimens under filament with a distance from the tungsten filament of 12 mm (Fig. 2a, b). This positioning choice is justified by a previous work [21] which assessed that samples located between filaments, after tribological tests, gives higher wear values of the diamond coating compared to the specimens positioned under filament. This result is ascribed to the lower quality of the diamond in terms of quality of the crystal lattice, and justified from the higher peak obtained in the Raman spectra.

Once established the positioning in the reactor, almost all the deposition parameters were constantly set according to the ones used in previous works [18, 19, 34], as shown in Table 3.

In particular, the only parameter that has been varied is the Methane/Hydrogen ratio with values of 1% and 2% as it affects the morphology of the deposited diamond. A low CH_4 concentration (1–2%) ensures that the carbon atoms are introduced in a controlled manner, allowing for the stable formation of the diamond structure. If the methane

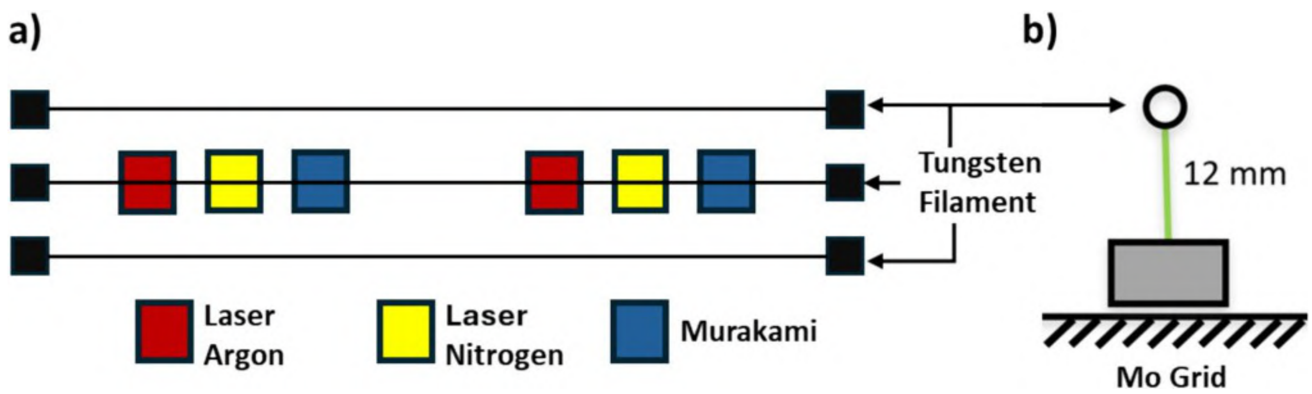

Fig. 2 Schematic of the positioning of the differently pre-treated WC–Co samples in the CVD reactor, in particular **a** top view; **b** front view

Table 3 Process parameters used for the HF-CVD diamond deposition on WC–Co substrate

Process parameters	Values
Pressure	10 mbar
Substrate temperature	680 °C
Filament temperature	2300 °C
Deposition time	14 h
CH_4/H_2	1–2%

Table 4 Analyzed pre-treatment/assistant gas ratio scenarios

Scenario ID	Pre-treatment technology	CH_4/H_2 ratio (for CVD deposition) (%)
1.1	Chemical etching	1
1.2	Chemical etching	2
2.1	Laser argon	1
2.2	Laser argon	2
3.1	Laser nitrogen	1
3.2	Laser nitrogen	2

concentration were higher, there could be an excess of carbon, leading to the formation of undesirable graphite or amorphous carbon [38]. Moreover, the right amount of H_2 helps regulate the substrate temperature, which is important for avoiding thermal damage to the WC–Co substrate, which has a lower melting point compared to diamond. Too much methane and insufficient hydrogen could lead to overheating or substrate degradation, negatively affecting the coating quality [39].

When pre-treatment with chemical etching occurs, the grain size of the deposited diamond changes from a micrometric structure to a nanometric cauliflower-like morphology [37, 40]. This effect is ascribed due to the massive "secondary" nucleation and a percentage increase in active species present in agreement with the literature. [40–42].

Summarizing, in total 6 different scenarios were investigated (ID and characteristics of each scenario underlined in Table 4), each one replicated three times in order to ensure reproducibility of the applied method and to have confirmation of subsequent results obtained.

2.2 Experimental Tests

After the diamond deposition on the samples, morphological and tribological analysis were performed to ensure the goodness of the coatings produced and to have a starting point for defining the tool life based on the comparison of the wears detected among the different pre-treatments and process parameters used.

From the Scanning Electron Microscopy (SEM) analysis shown in Fig. 3, is pointed out that the diamond films for all the considered scenarios are continuous and they uniformly cover the underlying WC–Co substrates. The main difference that can be observed through the SEM images, is the nanometric cauliflower structure obtained in case of scenario 1.2, confirming the results presented in other literature studies [37–39]. In all other cases, a similar microcrystalline structure is present, and the only differences to be noted between the 1% and 2% methane/hydrogen ratio with laser pre-treatments (scenarios 2.1 and 3.1 vs scenarios 2.2 and 3.2) relate to the greater presence of secondary growth as the percentage of methane increases. This phenomenon is attributable to the greater number of active species present during the deposition phase.

After ascertaining the proper adhesion of the coating by morphological analysis, dry linear reciprocating tribological tests were carried out using a Optimol SRV Tribometer. The counterpart consists of a 10 mm diameter WC-5.8%Co sphere, with a stroke of the reciprocating motion of 2 mm, frequency 50 Hz, and a total test duration of 10 min. The load applied to the specimens was initially set at 60 N, based on a previous literature work [21]. Unfortunately, by using this test configuration the nitrogen laser pre-treated

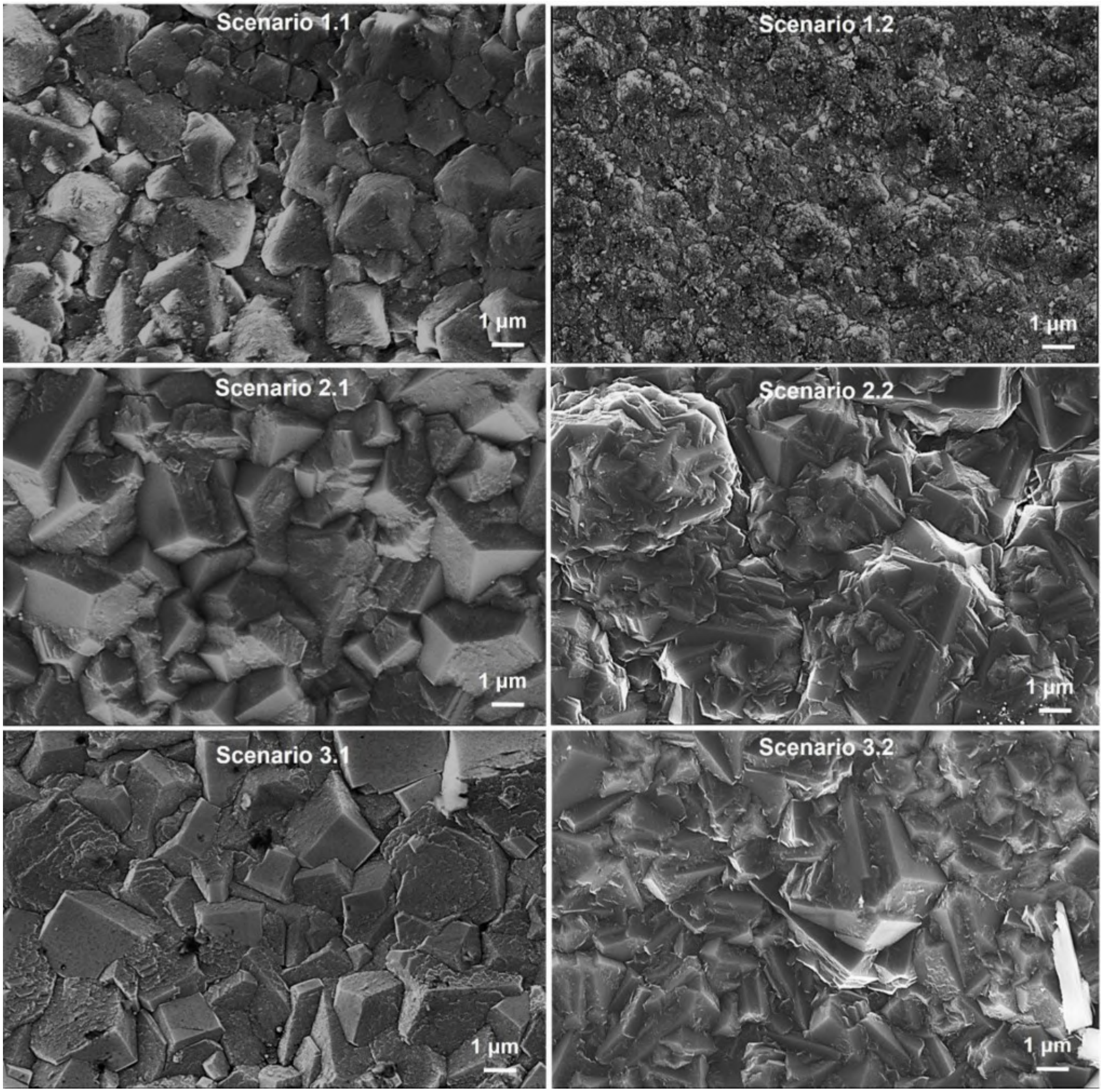

Fig. 3 SEM micrographs of diamond deposition on WC–Co substrate with the different types of pre-treatment analysed

specimens did not exhibit wear, consequently, needing a numerical wear volume to define the wear ratio that will later be used in the LCA study to define the service life for the different scenarios (see Sect. 3), it was chosen to increase the load to 70 N. After carrying out the wear tests, volume, dimension, and average depth of the wear tracks were obtained with the aid of the 3D profilometer Talysurf CLI 2000 by Taylor Hobson, equipped with an inductive probe with a diamond tip (radius of 2 µm). Further maps of the wear traces were acquired by covering all the traces on the samples, with a resolution of 3 µm on the x-axis, and 7 µm on the y-axis and were analysed using the features of the TalyMap software. Afterwards, a SEM acquisition of the wear traces was done in order to verify if the chosen load of 70 N imposed was sufficient to reach the substrate at the conclusion of the test.

The results of the wear tests are summarised in Fig. 4 and Table 5. From the 3D maps reported in Fig. 4, it can be noted that laser argon 1–2% pre-treated specimens (i.e. scenarios 2.1 and 2.2) show very obvious wear marks,

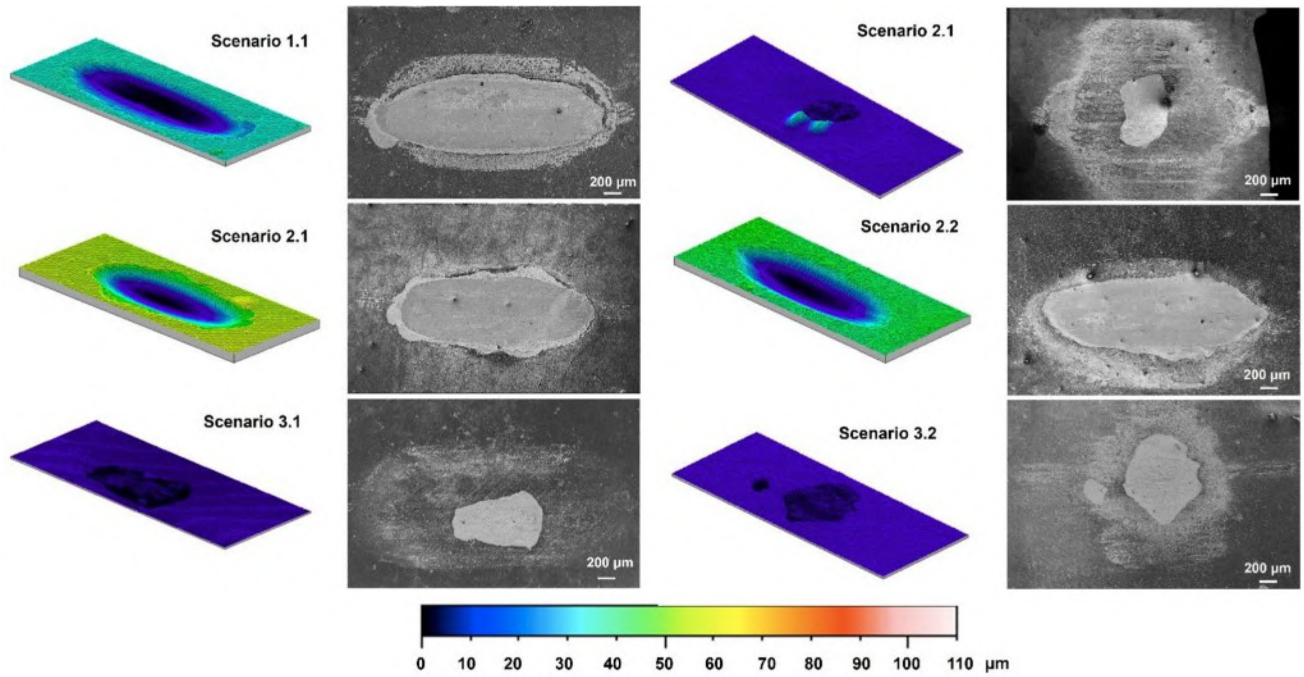

Fig. 4 3D maps and SEM images of the wear traces obtained from the tribological tests on the coated WC–Co samples

Table 5 Wear test results in terms of surface, volume, max and mean depth of the trace and wear ratio

Scenario	Surface of the trace (mm^2)	Volume of the trace (mm^3)	Max depth (μm)	Mean depth (μm)	Wear ratio (Wr)
1.1	4.53	0.0803	33.71	17.71	26.76
1.2	1.16	0.0030	10.10	2.60	1.00
2.1	1.17	0.0053	8.39	4.55	1.77
2.2	3.69	0.0099	11.10	2.68	3.29
3.1	4.16	0.1120	57.51	26.82	37.33
3.2	3.88	0.0859	44.21	22.21	28.63

attributable to the morphology of the diamond, as it has higher asperities as showed in Fig. 3 from the SEM images, becoming stress concentration zones when the film contacts the counterpart. From the SEM images in Fig. 4, substrate attainment was confirmed for all samples, highlighted by the lighter areas. The edges of the wear traces appear to be well defined and without coating delamination, thus it is possible to state for all specimens that the diamond films are well adhered throughout the entire duration of the wear tests. However, the difference in substrate exposure is evident between the samples pre-treated with Chemical etching 1%, Laser Argon 1–2%, and the samples pre-treated with Chemical etching 2%, Laser Nitrogen 1–2% which indicates that the adhesion of these latter samples is way higher than the former, attributable to the differences in the microstructure underlines and the reactivity of the Nitrogen onto the WC–Co substrate [35].

To numerically establish a reliable value that can give information on the actual wear and durability of the material in each scenario, to be used for the purpose of defining a common base of comparison in the LCA study, the wear ratio (Wr) parameter for each sample was defined using the following equation:

$$Wr_i = \frac{V_i}{V_{min}}$$

where V_i is the wear volume of the ith sample considered and V_{min} is the minimum wear volume obtained from the tests, represented by the value of 0.003 mm^3 obtained for the Chemical etching 2% sample (scenario 1.2).

The results reported in the following Table 5 confirm the previous outcomes derived from the morphological and tribological analyses: the Chemical etching 2% and Laser Nitrogen 1–2% scenarios show the lowest values of wear in terms of surface and volume of the trace.

3 Methods

The Life Cycle Assessment (LCA) is a robust analytical methodology standardized under the ISO 14040 and ISO 14044 standards [43, 44], widely recognized in environmental management systems. This method provides a holistic framework for evaluating the environmental impacts of a product, process, or service throughout its entire life cycle—from raw material extraction through processing, use, and disposal or recycling (cradle-to-grave approach). Guided by the aforementioned standards, LCA research is structured around four essential phases:

1. *Goal and Scope Definition* The initial phase of an LCA involves setting clear objectives for the analysis. It is crucial to define the functional unit, which quantifies the performance of the product system for use as a reference, and establish precise spatial and temporal boundaries. This phase ensures that the study is aligned with its intended purpose and contextual limits.
2. *Life Cycle Inventory (LCI)* This phase constitutes the core of the LCA process. The system under analysis is broken down into its constituent unit processes. An input–output analysis is then conducted for each process to capture and categorize all relevant flows within the system boundaries. This stage is critical for collecting comprehensive data that forms the basis for the subsequent impact assessment.
3. *Life Cycle Impact Assessment (LCIA)* In this step, the collected data from the LCI are translated into potential environmental impacts. This transformation is achieved through the application of specific impact assessment methodologies that utilize characterization and weighting factors. These methodologies help in delineating the impact of the system in both midpoint and endpoint categories, providing a clearer picture of environmental performance.
4. *Results Interpretation* The final phase involves a thorough analysis and critical review of the results obtained from the LCIA. This step is crucial for interpreting the data in the context of the defined goals and scope. It also includes a review of the LCA process and its outcomes, fostering a better understanding of the system's environmental impacts and identifying opportunities for improvement.

Each of these phases is interconnected, forming a comprehensive framework that supports the detailed analysis of environmental impacts associated with any given product system. The following subsections will delve into the specifics of the goal and scope definition and the LCI, while detailed discussions on the results and subsequent interpretations will be presented in Sect. 4.

3.1 Goal of the Study and Functional Unit

The main goal of this study is to analyze the environmental impact of the entire process HF-CVD diamond coating deposition to determine which phases are the most impactful. More specifically, the study aims to comparatively evaluate different scenarios, characterized by the three alternative pre-treatment processes (chemical etching and laser treatments with different assistant gas), as illustrated in the previous Sect. 2. This research arises because the most widely used industrial pretreatment prior to the diamond deposition of the WC–Co substrate is chemical etching, which requires special care in storage, handling, and disposal of the chemical substances involved, while the laser pre-treatment appears safer.

The main functional unit for this study is defined as "the realization of a diamond surface coating on a tungsten carbide (WC–Co) sample with the physical characteristics and mechanical performance as illustrated in Table 1, including different alternatives for the surface preparation and the deposition phases, and considering differentiated service lives for each production scenarios. This allows for the assessment and comparison of environmental impacts under different production scenarios, as detailed in Sect. 2 (Table 4). The reference flow encompasses all material and energy inputs needed for conducting the specified surface treatments and subsequent diamond deposition processes. This includes not only the direct materials involved in the coatings and treatments but also ancillary materials and energies, such as chemicals for pre-treatment, gases for deposition processes, electricity for machinery, and any other resources essential for modelling the complete lifecycle of the WC–Co sample with a diamond coating.

For the purpose of comparing in details the three alternative pre-treatment processes (i.e. chemical etching and lasers), a "secondary" functional unit has been defined as "the pre-treatment of a tungsten carbide (WC–Co) sample with the physical characteristics as illustrated in Table 1, to be successively used for diamond coating deposition."

3.2 Description of the System Boundaries

In this LCA study, various scenarios involving different pre-treatment methods followed by varying deposition conditions are assessed to determine their environmental impacts on WC–Co samples. The scenarios are classified

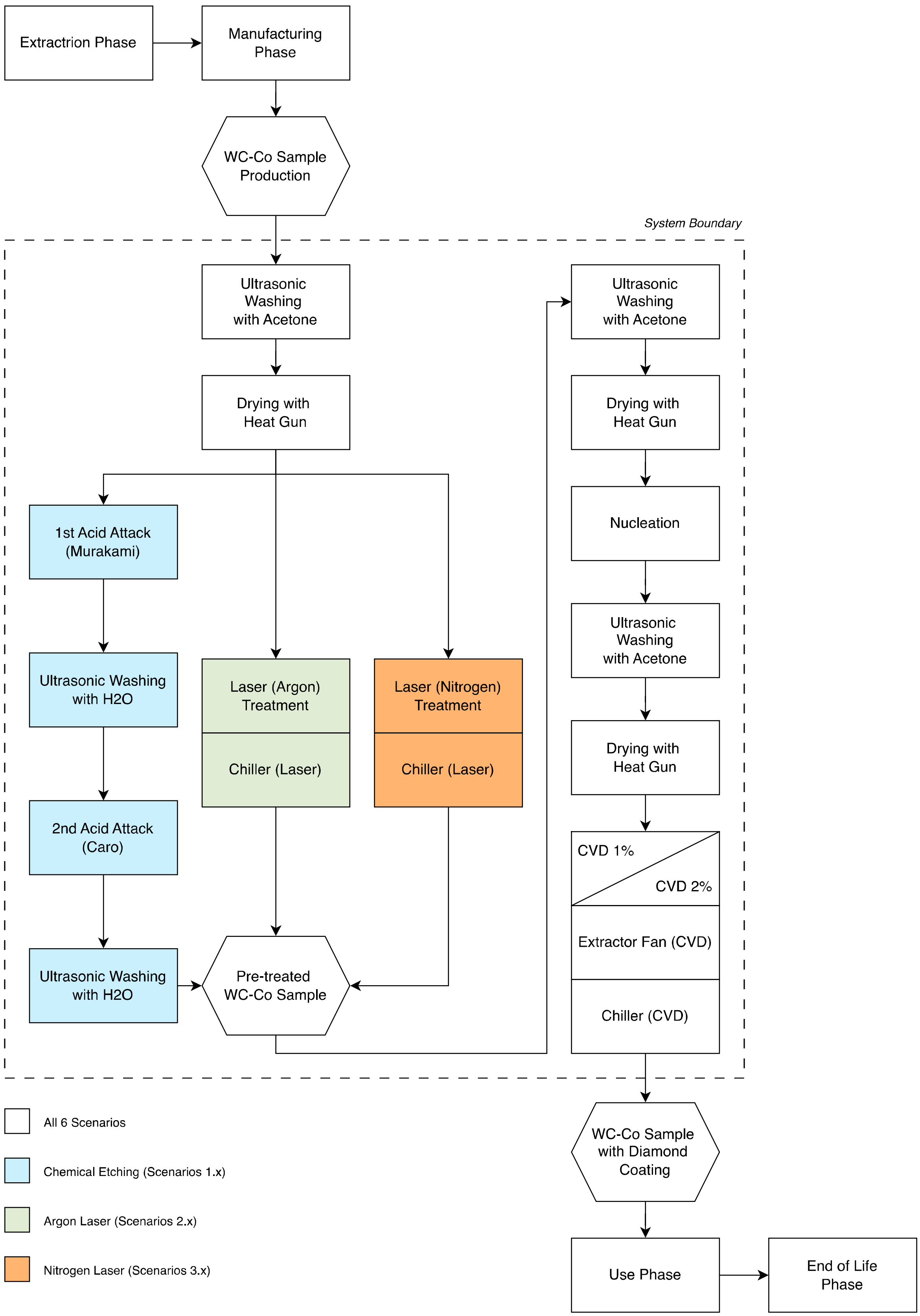

Fig. 5 Comprehensive system boundaries of all the analyzed scenarios: common phases (white), scenarios 1.x (blue), scenarios 2.x (green), scenarios 3.x (orange)

in Table 4, while the following Fig. 5 illustrates the system boundaries, as well as the sub-phases included in each scenario that have guided the LCA model building.

The system boundaries for this LCA are defined to exclusively focus on the pre-treatment and deposition stages of WC–Co platelets, according to a gate-to-gate approach. This specification allows the environmental assessment to concentrate on the variations introduced by different pre-treatment methods, which constitute the primary focus of this comparative analysis. As depicted in Fig. 5, the production of the WC–Co samples itself, its use, and end-of-life phases are excluded from this analysis, as these stages remain constant across all scenarios and do not influence the assessment outcomes of the pre-treatment and deposition processes. Precisely, the system boundary is composed as follows:

- *Input Boundary* All raw materials, chemicals, and energy inputs required for executing each pre-treatment and deposition scenario are included. This encompasses everything from the chemicals used in the double chemical attack to the gases employed in the CVD processes under varying methane-to-hydrogen ratios.
- *Core Processes* The focus is placed specifically on the pre-treatment techniques (chemical or laser) and the CVD. Energy and material consumptions are tracked, reflecting the environmental impacts evaluated within the gate-to-gate scope.
- *Output Boundary* All direct emissions, waste products, and potential recycling outputs generated from the pre-treatment and deposition stages are captured. Downstream end-of-life management activities, such as recycling or final disposal of the WC–Co sample, are excluded from the current system modeling, as they remain constant across all scenarios and do not impact the comparative evaluation of the pre-treatment and deposition processes.

3.3 Life Cycle Inventory (LCI)

The LCI conducted in this study thoroughly documents the collection of data from a combination of direct experimental measurements, referenced scholarly articles, and secondary data sourced from the Ecoinvent 3.6 database. This comprehensive approach ensured that the LCI encompassed detailed material and energy flow information within the specified system boundaries of the manufacturing process for diamond-coated tungsten carbide samples (Table 6).

The following assumptions have been made to collect the relevant inventory data:

- Data related to input materials/substances for the chemical etching, laser treatments, CVD depositions, and ultrasonic washings (e.g. used chemical substances, gases for lasers, gases for CVD chamber) have been collected by measuring the quantities used in the experiments;
- Electric energy consumption related to laser treatments, CVD depositions, and CVD chiller have been measured during the experiments through a network analyzer. Concerning the CVD phase, the measured electric energy consumptions for chiller and deposition are related to the full set of 70 samples jointly treated within the CVD reactor, thus the energy consumptions considered in the study for each sample has been derived by dividing the measured consumptions per number of samples treated in a CVD cycle;
- Electric energy consumption related to laser chillers, drying gun and extractor fan have been estimated on the basis of the nominal powers of equipment and duration of the different treatments;
- Inventory data related to input materials (except potassium ferrocyanide and diamond powder) and electric energy generation have been derived from the Ecoinvent 3.6 database;
- Due to the unavailability of both primary and secondary LCI data from Ecoinvent, the production of potassium ferricyanide and diamond powder has been modelled on the basis of relevant literature studies (see Sects. 3.3.1 and 3.3.2);
- Impacts related to the manufacturing of machines and equipment used during the pre-treatments and depositions (i.e. laser equipment, CVD reactor) are considered negligible, since their service lives are much larger than the temporal boundaries of the analysis (i.e. pre-treatment and deposition of one single sample), as demonstrated in other LCA studies related to manufacturing processes [45];
- According to the system boundaries, WC–Co sample production, use, and end-of-life are not considered in the LCA model.

3.3.1 Murakami Sub-reagents Modelling

The modeling of the Murakami acid treatment posed significant challenges due to the unavailability of three key sub-reagents in the Ecoinvent 3.6 database. To address this, detailed modellings, described in Table 7, were based on external references as follows:

- Potassium ferricyanide synthesis was based on a specific patent [46], providing the necessary procedural details.
- Potassium ferrocyanide, needed to produce potassium ferricyanide, was modeled using data from two sources [47], detailing the necessary reagents and quantities.

Table 6 LCI Data for all the analyzed phases

Phase	Flow	Quantity
Ultrasonic washing with acetone	Electric energy	20 Wh
	Acetone	3.92 g
	Waste incineration (acetone)	3.92 g
Drying with heat gun	Electric energy	63 Wh
1st acid attack (murakami)	Electric energy	30 Wh
	Murakami acid	0.50 g
	Sodium cyanide	4.99 g
	Deionized water	0.50 g
	Potassium ferricyanide	
	Waste incineration (murakami acid)	5.99 g
Ultrasonic washing with deionized H_2O	Electric Energy	30 Wh
	Deionized Water	130 g
	Wastewater Treatment (Deionized Water)	0.13 l
2nd acid attack (Caro)	Electric Energy	0.33 Wh
	Caro acid	0.27 g
	Sulfuric acid	4.84 g
	Hydrogen peroxide	
	Waste incineration (Caro Acid)	5.15 g
Laser (argon) treatment	Electric energy	54.2 Wh
	Argon	4.05 g
	Gas released (argon)	4.05 g
Laser (nitrogen) treatment	Electric energy	54.2 Wh
	Nitrogen	2.84 g
	Gas released (nitrogen)	2.84 g
Chiller (laser)	Electric energy	20 Wh
Nucleation	Electric energy	30 Wh
	Diamond powder	0.0026 g
	Ethanol	0.21 g
	Waste incineration (ethanol)	0.21 g
CVD with CH_4/H_2 ratio = 1%	Electric energy	1803.04 Wh
	Hydrogen	7.88 g
	Methane	0.48 dm^3
	Gas released (hydrogen)	7.88 g
	Gas released (methane)	0.63 g
CVD with CH_4/H_2 ratio = 2%	Electric energy	1803.04 Wh
	Hydrogen	7.88 g
	Methane	0.96 dm^3
	Gas released (hydrogen)	7.88 g
	Gas released (methane)	1.25 g
Extractor fan (CVD)	Electric energy	5.8 Wh
Chiller (CVD)	Electric energy	366.36 Wh

Iron rust powder was substituted with iron pallets, as suggested by Wilfong et al.[32], to enable the production of potassium ferricyanide [46].

- Calcium formate, another critical component, was modeled using a balanced chemical formula from an online source [48], allowing precise mass calculations of the required elements.

3.3.2 Diamond Powder Modelling

The nucleation process prior to the HF-CVD deposition involved the use of diamond powder, which was not available in the reference LCI database, i.e. the Ecoinvent 3.6. To model this material, the production of diamond powder was based on graphite, following the methodology described in [31]. The mass required for nucleation was determined from the concentration of diamond in ethanol,

Table 7 Murakami acid's sub-reagents LCI

Murakami sub-reagents	Flow	Quantity
Potassium ferricyanide (1 kg)	Thermal energy	21.6 MJ
	Potassium ferrocyanide	1.43 kg
	Deionized water	1.53 kg
	Potassium hydroxide	0.031 kg
	Lime	0.031 kg
	Calcium formate	0.043 kg
Potassium ferrocyanide (1 g)	Thermal energy	2.70 MJ
	Sodium carbonate	0.40 g
	Charcoal	0.40 g
	Rust powder	0.20 g
	Potassium hydroxide	1 g
Calcium formate (1 g)	Calcium carbonate	0.77 g
	Formic acid	0.71 g
	Gas emission (carbon dioxide)	0.34 g

which is 50 ct/l, and the conversion factor of carats to grams (1 ct = 0.2 g) [20]. These values were utilized to calculate the quantities necessary for producing 1 kg of diamond powder. Additionally, the thermal energy required for this production process was quantified at 3024 MJ[31].

3.3.3 Samples Service Life

According to the experimental tests described in Sect. 2.2, the samples prepared following the 6 considered pre-treatments and deposition scenarios exhibited not homogeneous performances in terms of wear. Considering the most widely industrial usage of the diamond coated WC–Co inserts for machining tools, the wear volume can be strictly correlated with the service life of the samples, so was not possible to make a simple 1 vs 1 LCA comparison between the analysed scenarios.

Therefore, on the basis of the calculated wear ratio parameter (see the values for each scenario in Table 5), the Scenario 1.2 sample has been assumed as the reference one, since it has the lowest wear value and potentially the highest service life duration. In a purely comparative manner for the other scenarios, has been made the hypothesis that to cover the same service life duration guaranteed to the reference case (i.e. Scenario 1.2 sample) a number of samples corresponding to the wear ratio are needed for each scenario. Such assumption allowed to guarantee the same functional unit for each considered sample and thus have been used within the LCA model to adequately compare the analyzed scenarios.

3.4 Life Cycle Impact Assessment (LCIA) Methods

In assessing the environmental impact throughout the life cycle of the studied products, it is essential to select a robust and comprehensive LCIA methodology. The choice of an LCIA method can significantly influence the outcomes and interpretations of an environmental assessment. In this study, the ReCiPe methodology was utilized for the LCIA due to its comprehensive approach to evaluating multiple environmental impacts, as supported by other studies focused on the LCA of manufacturing processes [49].

The ReCiPe method [50] is well-regarded for transforming extensive life cycle inventory data into a limited number of impact scores, which represent the relative severity of various environmental issues. It provides two levels of indicators: midpoint and endpoint. Midpoint indicators, such as Global Warming Potential (GWP) [kg CO_2 eq], Freshwater Eutrophication [kg P eq], and Terrestrial Acidification [kg SO_2 eq], measure environmental mechanisms directly linked to the product system. Endpoint indicators, on the other hand, translate these midpoints into three broader categories of damage: Human Health [Pt], Ecosystems [Pt], and Resources [Pt], thus providing a more holistic view of potential environmental damages.

The selection of the ReCiPe methodology was based on its inclusion of a wide range of impact categories, which align well with the complex nature of environmental impacts involved in the manufacturing of diamond-coated tools. This method is particularly effective in accounting for diverse environmental impacts beyond just the single impact category, ensuring a comprehensive assessment as suggested by current literature and standards within the sector [51]. Such an approach not only addresses direct emissions but also incorporates a broader spectrum of environmental impacts, providing a multi-faceted view of sustainability.

The methodology was applied using the Hierarchist (H) perspective for midpoint indicators and the Average (A) perspective for endpoint indicators. This choice was motivated by the balanced approach of the Hierarchist perspective, which is designed to mediate between precautionary and optimistic viewpoints, making it suitable for scenarios involving significant scientific uncertainty [52] The average perspective for endpoints aids in providing a generalized view across different environmental impacts, facilitating more informed decision-making [53].

However, a focus on GWP indicator has been made since it is largely considered the most adopted, widespread and understandable environmental metric to assess the environmental performance of products and manufacturing processes [54]. This study considered the methodology described in the Fifth Assessment Report (2013) of Intergovernmental Panel on Climate Change (IPCC) [55] which accounts the greenhouse contribution of each flow in comparison with the carbon dioxide, assumed as reference flow, and in a time horizon of 100 years.

4 Results and Discussion

In this section, the results of the LCIA calculated using the LCI data and the selected environmental impact categories are presented. The modelling and analysis, conducted using the SimaPro 9.4.0.2 software tool equipped with the EcoInvent 3.6 database, aims to elucidate the environmental impacts associated with different scenarios of diamond coating deposition processes. In particular, the comparison between traditional chemical pre-treatment methods and innovative laser treatments is highlighted to understand their respective environmental burdens. The following subsections provide detailed findings from the ReCiPe midpoint calculations, with a particular focus on the GWP indicator, and the ReCiPe endpoint evaluation. The assessment considers the main functional unit and takes into account wear performance to consider the service lives. Additionally, an in-depth comparison of the pre-treatment processes is included, using the secondary functional unit to focus on the specific impacts of each pre-treatment method, considering a simple 1 vs 1 comparison and excluding the service lives for each scenario.

4.1 ReCiPe Midpoint Analysis

The ReCiPe midpoint impact assessment results, calculated using the Hierarchist (H) version for Europe, are critical for understanding the environmental implications of each process in a comprehensive way, considering different impact categories and deeply understanding the causes of impacts. The obtained results are detailed in Table 8 and represented in Fig. 6 and "Appendix" of the paper. The table provides a detailed quantitative comparison of the results in terms of ReCiPe midpoint indicators for each scenario, with the identification of the most impactful (italic boxes) and most sustainable (bold boxes) options for each scenario. The graph in Fig. 6, instead, visually highlights the relative impacts across different categories using normalized values, where the most impactful scenario in each category is scaled to 100%, and all other scenarios are proportionally represented. Finally, "Appendix" also reports the relative contributions of processes for the six scenarios, useful to identify the critical flows, which generally result from the chemical-based pre-treatments, and the CVD processes (i.e. deposition phase).

From a general perspective, Scenario 2.1 stands out with notable impacts compared to other scenarios. Factors contributing to this include its very high wear ratio of 37.3 (i.e. very short service life), which necessitates more frequent replacements during a hypothetical application of the sample as a tool, and thus amplifies the cumulative environmental impacts over time. Electricity usage for the energy-intensive CVD process is the major contributing

Table 8 LCIA in terms of each characterized ReCiPe Midpoint H for each scenario (bold: least impactful; italic: most impactful)

Midpoint indicator	Scenario 1.1	Scenario 1.2	Scenario 2.1	Scenario 2.2	Scenario 3.1	Scenario 3.2
Global warming (kg CO_2 eq)	3.68E+01	**1.40E+00**	*3.99E+01*	3.13E+01	1.92E+00	3.59E+00
Stratospheric ozone depletion (kg CFC11 eq)	1.97E−05	**7.34E−07**	*2.41E−05*	1.85E−05	1.16E−06	2.13E−06
Ionizing radiation (kBq Co-60 eq)	2.46E−01	**9.17E−03**	*3.23E−01*	2.48E−01	1.53E−02	2.80E−02
Ozone formation. Human health (kg NO_x eq)	5.41E−02	**2.02E−03**	*6.70E−02*	5.14E−02	3.22E−03	5.90E−03
Fine particulate matter formation (kg PM2.5 eq)	3.44E−02	**1.29E−03**	*4.35E−02*	3.34E−02	2.09E−03	3.83E−03
Ozone formation. Terrestrial ecosystems (kg NO_x eq)	5.55E−02	**2.07E−03**	*6.86E−02*	5.26E−02	3.29E−03	6.04E−03
Terrestrial acidification (kg SO_2 eq)	9.97E−02	**3.72E−03**	*1.28E−01*	9.79E−02	6.13E−03	1.12E−02
Freshwater eutrophication (kg P eq)	1.47E−03	**5.49E−05**	*1.68E−03*	1.29E−03	8.01E−05	1.47E−04
Marine eutrophication (kg N eq)	*1.74E−04*	6.48E−06	1.07E−04	8.22E−05	**5.13E−06**	9.41E−06
Terrestrial ecotoxicity (kg 1.4-DCB)	9.11E+01	**3.40E+00**	*1.17E+02*	8.95E+01	5.62E+00	1.03E+01
Freshwater ecotoxicity (kg 1.4-DCB)	*3.29E−02*	1.23E−03	1.72E−02	1.32E−02	**8.26E−04**	1.51E−03
Marine ecotoxicity (kg 1.4-DCB)	*1.00E−01*	**3.73E−03**	9.26E−02	7.11E−02	4.46E−03	8.18E−03
Human carcinogenic toxicity (kg 1.4-DCB)	4.86E−01	**1.81E−02**	*5.01E−01*	3.84E−01	2.41E−02	4.42E−02
Human non-carcinogenic toxicity (kg 1.4-DCB)	7.28E+00	**2.72E−01**	*8.73E+00*	6.70E+00	4.20E−01	7.70E−01
Land use (m2a crop eq)	8.23E−01	**3.07E−02**	*1.05E+00*	8.09E−01	5.06E−02	9.29E−02
Mineral resource scarcity (kg Cu eq)	6.03E−02	**2.25E−03**	*7.48E−02*	5.74E−02	3.60E−03	6.60E−03
Fossil resource scarcity (kg oil eq)	1.08E+01	**4.02E−01**	*1.23E+01*	9.40E+00	5.89E−01	1.08E+00
Water consumption (m^3)	5.24E−01	**1.96E−02**	*6.98E−01*	5.35E−01	3.32E−02	6.08E−02

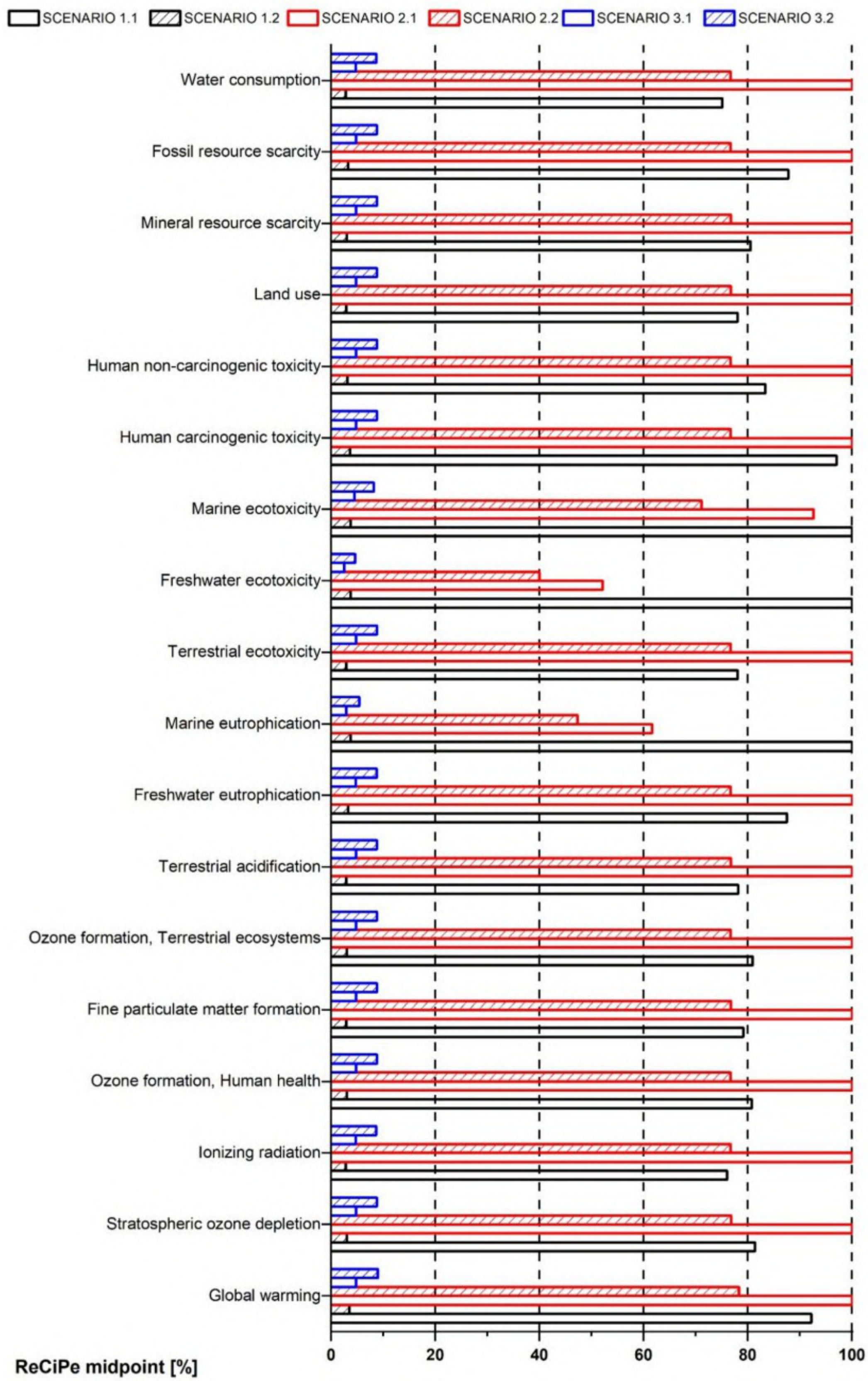

Fig. 6 LCIA in terms of characterized ReCiPe Midpoint H (normalization applied)

factor to the impacts on the indicators. The significant energy demand of the CVD process, to maintain the high temperatures necessary for the deposition process and to support ancillary systems, exacerbates these impacts, a well-known issue within the field [56–58].

Following Scenario 2.1, the scenarios can be ranked in terms of environmental impact as follows: 1.1, 2.2, 3.2, 3.1, with 1.2 being the least impactful overall. This ranking reflects the order from the least resistant to the most resistant in wear tests, corresponding to the samples with the shortest to the longest service life.

Some non-aligned results can be observed for the indicators Marine Eutrophication, Freshwater Ecotoxicity and Marine Ecotoxicity for which Scenario 1.1 turned out to be the worst solution, instead of Scenario 2.1 (second worst solution for all three cases). The reasons for this are multifaceted. First, the short service life of the components necessitates multiple replacements, leading to repeated cycles of the same environmentally detrimental processes. The chemical etching process involves the use of hazardous chemicals like Murakami and, particularly, Caro acid, which significantly impacts these three indicators due to their high toxicity and contribution to ecotoxicity. Indeed, besides the electricity consumption in the CVD process, the most influential flows affecting the three considered midpoint indicators (i.e. Marine Eutrophication, Freshwater Ecotoxicity, and Marine Ecotoxicity) are the use of potassium ferricyanide in Murakami acid and the waste treatment required for Caro acid. The high toxicity of potassium ferricyanide is well-documented, posing significant risks to aquatic ecosystems even at low concentrations. This compound can release free cyanide ions under certain conditions, which are highly toxic to aquatic organisms. The oxidative properties of potassium ferricyanide can lead to oxidative stress, disrupting cellular functions and causing substantial damage to aquatic life, as evidenced by studies such as those conducted by Garg and Singh [59]. The waste treatment of Caro's acid, specifically the handling of potassium peroxymonosulfate (Oxone), significantly exacerbates environmental impacts due to its generation of reactive oxygen species (ROS). These ROS can lead to oxidative stress in aquatic organisms, causing cellular damage and impairing metabolic processes [60].

Scenario 2.2, although, utilizing 2% for the CH_2/H_4 ratio during CVD deposition, instead of 1% as in Scenario 2.1, benefits from this difference with the sensible increase of the service life of the sample by 23.32%, thereby significantly reducing the environmental impacts.

Scenarios 3.1 and 3.2 both employ laser treatment with nitrogen and demonstrate moderate impacts. The sample in Scenario 3.1 is 45.45% more resistant in terms of wear, as demonstrated by the value in Table 5, compared to the sample in Scenario 3.2, which also uses CVD 1% instead of CVD 2%. These differences, in the context of moderate impacts, significantly affect their respective environmental footprints. Scenario 3.1 achieves the best performance in Marine Eutrophication and Freshwater Ecotoxicity due to its lower overall energy consumption and the effectiveness of its nitrogen laser treatment in minimizing emissions. This finding is consistent with studies highlighting the lower environmental impact of laser treatments in material processing [61].

Scenario 1.2 emerges as the least impactful, with the lowest values across most of the indicators (16 on a total of 18). Despite sharing all the processes executed in Scenario 1.1, which ranks as one of the worst due, Scenario 1.2 benefits from an increased methane-to-hydrogen ratio of 2%, improving the sample's service life by 26.8 times. This enhancement mitigates the individual impacts of the processes that are particularly detrimental in Scenario 1.1. The observed exceptions are in the Marine Eutrophication and Freshwater Ecotoxicity midpoint categories where Scenario 3.1 excels due to the avoided use of the chemical-based pre-treatments that are particularly critical for impact related to eutrophication and toxicity of water, as discussed above [59].

4.2 Global Warming Potential Analysis

GWP quantifies the contribution of a system to global warming and climate change, according to the methodology defined by the IPCC, and is widely accepted as one of the most used and understandable environmental indicators in the field of sustainable manufacturing. The performance of the various scenarios regarding GWP, as illustrated in Fig. 7, follows the general trend described in the previous section. A clear conclusion can be taken about the most critical scenario: the impacts of Scenario 2.1 (39.9 kg CO_2 eq) are significantly higher compared to all the other scenarios: + 8.4% compared to Scenario 1.1 (36.8 kg CO_2 eq), + 27.5% compared to Scenario 2.2 (31.3 kg CO_2 eq), + 1011.4% compared to Scenario 3.2 (3.59 kg CO_2 eq), + 1980.73% compared to Scenario 3.1 (1.92 kg CO_2 eq), and + 2750% compared to Scenario 1.2 (1.4 kg CO_2 eq).

In detail, the most significant contributors to GWP are the electricity consumption for the CVD process and for cooling systems (Chiller CVD) to maintain optimal operational conditions during the deposition phase. This emphasizes the importance of energy efficiency for mitigating GWP in manufacturing operations. Among the processes, the aspirator CVD is the least impactful due to its reduced power rating. Comparing 1 vs 1 the CVD 1% and CVD 2%, which differentiates only for the CH_4/H_2 ratio used within the deposition chamber during the deposition phase, their impact in terms of GWP is very

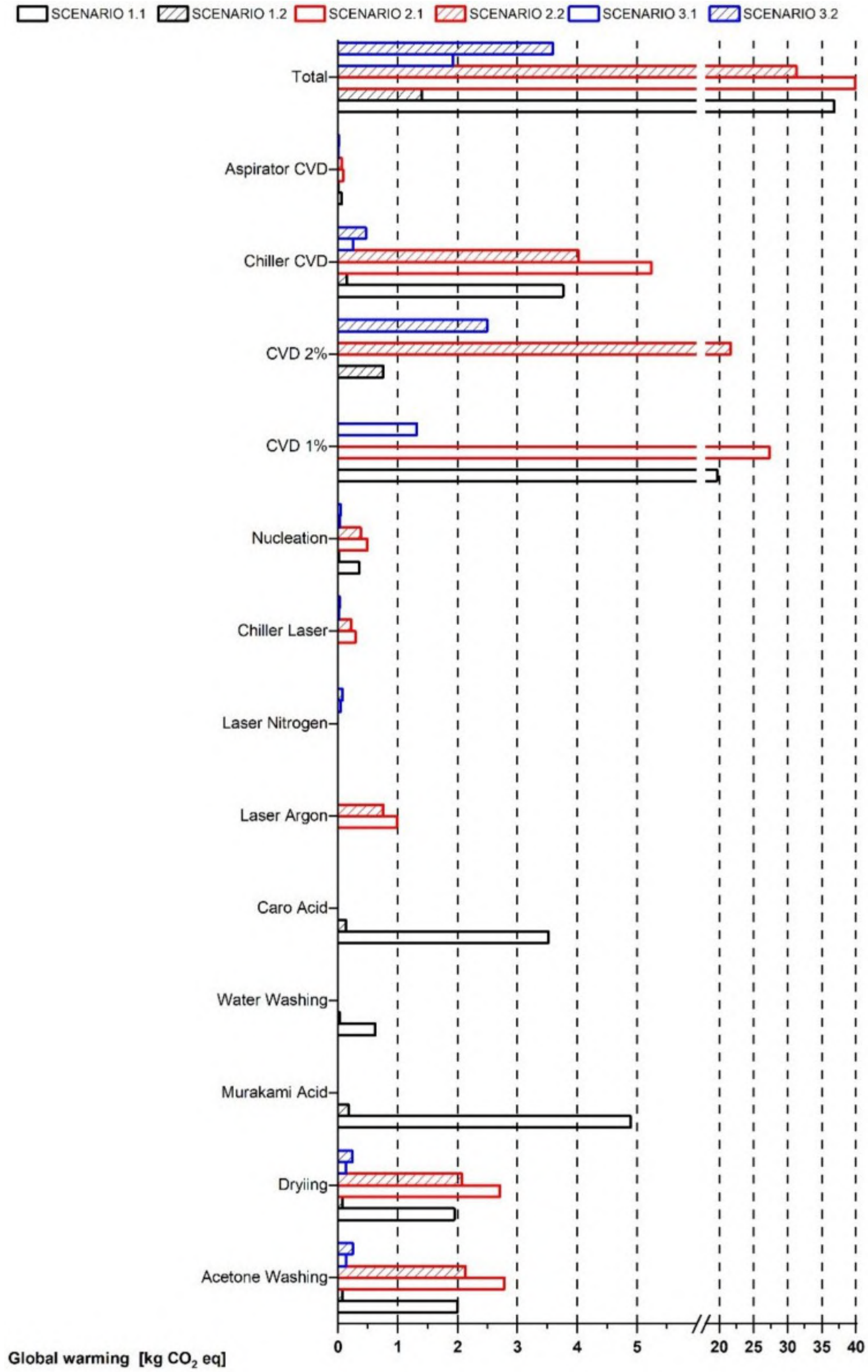

Fig. 7 LCIA in terms of global warming potential (GWP) for each scenario, with details on the split of contributions for each sub-phase

similar, with CVD 1% having a 2.31% lower impact. However, the difference lies in how they contribute to extending the samples' service lives. CVD 2% tends to significantly improve lifespan in scenarios involving chemical etching and laser argon pre-treatments. This is likely due to the increased methane-to-hydrogen ratio, which enhances the deposition process, leading to a more durable film. Conversely, the specific interaction between the nitrogen laser treatment and the deposition process does not benefit as much from the increased methane-to-hydrogen ratio, resulting in better performance when using CVD 1%. Moreover, the Murakami acid process, particularly the use of potassium ferricyanide, the electricity required, and the management of its waste products further aggravate GWP impacts in the case of Scenario 1.1.

4.3 ReCiPe Endpoint Analysis

The ReCiPe endpoint method, utilizing the Hierarchist (H) version for Europe with the average weighting set (A), consolidates midpoint impact categories into three overarching endpoint categories: Human Health, Ecosystems, and Resources. This approach provides a comprehensive overview by weighing and normalizing the midpoint results to yield a single score, facilitating the assessment of overall environmental performance and making it easier to identify which scenarios are more sustainable.

The ReCiPe endpoint results corroborate the trends observed in the midpoint analysis. Notably, Scenario 1.2 remains the least impactful, with a total endpoint indicator impact of 4.01E+01 mPt. This scenario demonstrates reduced damage of – 32% compared to Scenario 3.1 (5.89E+01 mPt), – 63.3% compared to Scenario 3.2 (1.09E+02 mPt), – 95.8% compared to Scenario 2.2 (9.52E+02 mPt), – 96.2% compared to Scenario 1.1 (1.06E+03 mPt), and – 96.7% compared to Scenario 2.1 (1.23E+03 mPt).

A detailed analysis reveals that the most critical damage category is Human Health, followed by minimal damages in terms of Ecosystem and Resource, as shown in Fig. 8.

In terms of Human Health, the primary contributing factors are emissions that affect air quality, toxicological effects from chemical use, and energy-related impacts. The energy-intensive processes result in substantial emissions of greenhouse gases and air pollutants, which contribute to respiratory and cardiovascular diseases. Studies indicate that exposure to PM2.5 and NOx is linked to an increased risk of hospital admissions for respiratory and cardiovascular conditions, as well as chronic illnesses such as COPD and lung cancer [62, 63].

The highly toxic chemical processes pose severe risks to human health through exposure and contamination of water sources. Similarly, the waste treatment of acids involves managing hazardous substances, in particular, the hydrogen peroxide and potassium peroxymonosulfate of Caro Acid, which can generate reactive oxygen species, leading to oxidative stress and cellular damage. Studies have shown that long-term exposure to the emissions and chemical byproducts associated with these processes can lead to chronic health issues such as cancer, neurological disorders, and reproductive toxicity [64].

The heavy reliance on fossil fuels for electricity generation further exacerbates these health impacts by contributing to climate change, which is associated with a wide range of health risks including heat-related illnesses, vector-borne diseases, and food security challenges [65].

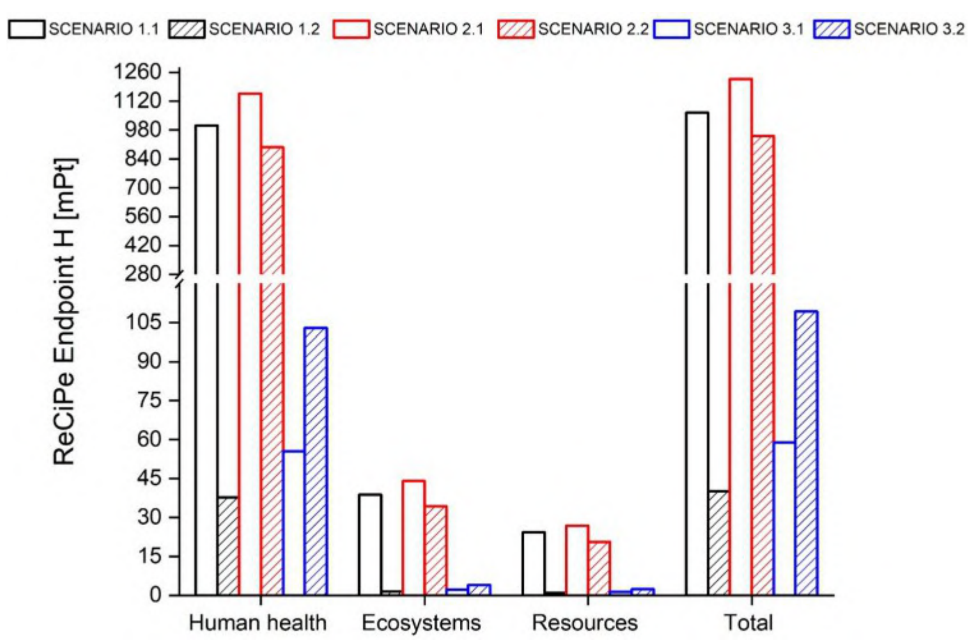

Fig. 8 LCIA in terms of ReCiPe endpoint H for each scenario, with the split of contributions in terms of each damage category

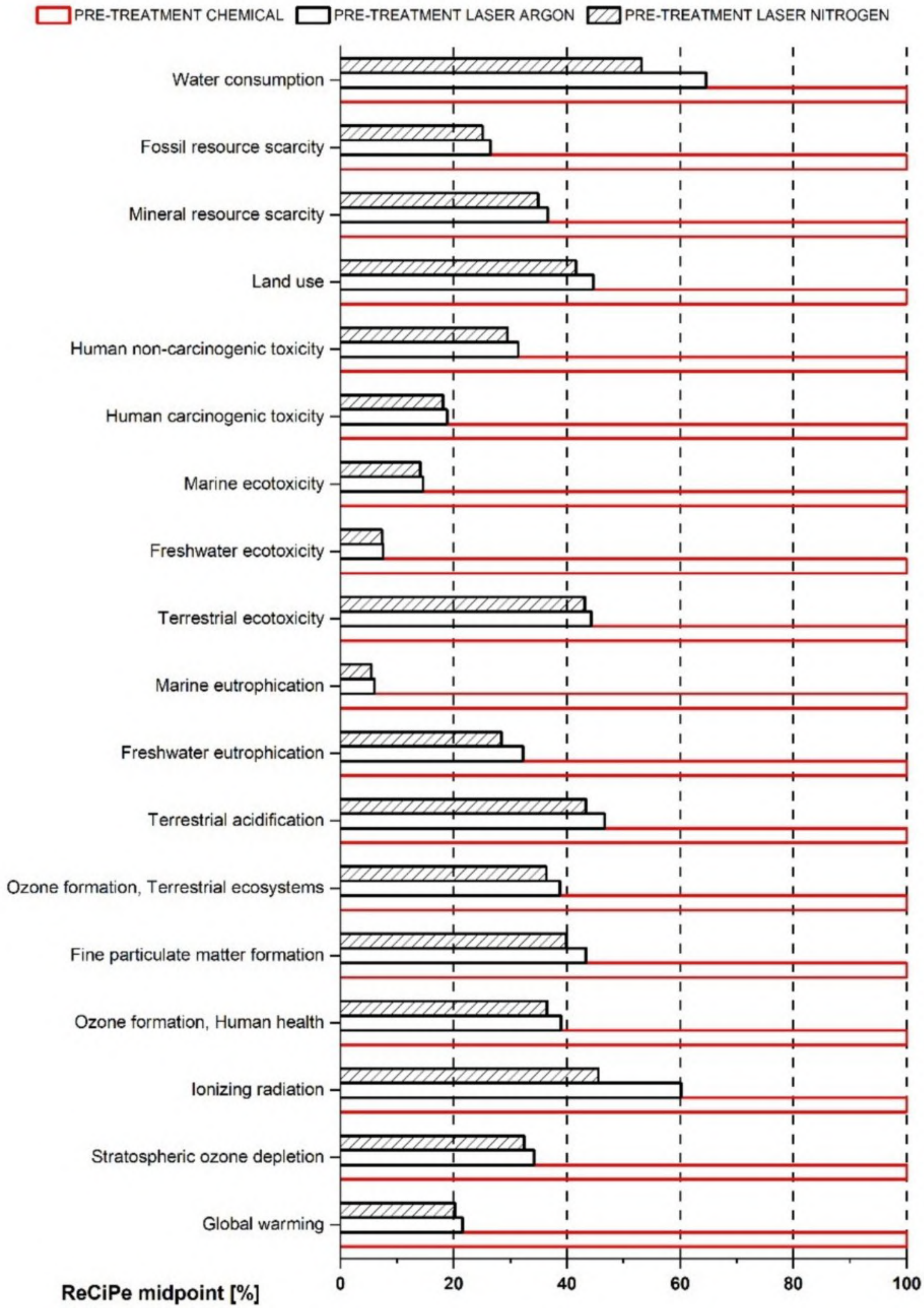

Fig. 9 Detailed comparison among pre-treatment considering ReCiPe Midpoint H indicators (normalization applied)

4.4 Details on Pre-treatment Processes

In this section, a detailed analysis of the pre-treatment of a WC–Co sample using the secondary functional unit is illustrated. The primary functional unit used previously incorporated the service life of each sample (i.e. wear performance), significantly influencing the final impacts of the scenarios. This analysis, instead, is necessary to understand the specific impacts of each pre-treatment process, since it allows for the isolation and evaluation of the environmental burdens of the pre-treatment processes themselves.

As shown in Fig. 9, the chemical pre-treatment process demonstrates a considerably higher environmental impact compared to laser treatments in all the considered indicators (i.e. ReCiPe midpoints). Analyzing the data, Water Consumption shows the smallest difference in impact, with laser argon reducing it by 35.4% and laser nitrogen by 46.9% compared to chemical pre-treatment. Conversely, the largest difference is observed in Marine Eutrophication, where laser argons reduce the impact by 94% and laser nitrogen by 94.6% compared to chemical pre-treatment. These findings highlight the potential of laser nitrogen treatments as a more environmentally sustainable alternative to both chemical pre-treatments and laser argon treatments. The difference between the two laser pre-treatments lies primarily in the distinct characteristics of the gases used. Argon, a noble gas with a higher density (approximately 1.784 g/L at 0 °C and 1 atm) compared to nitrogen (1.251 g/L at 0 °C and 1 atm), occupies a smaller volume per unit mass [59]. However, to achieve the same operational conditions in the laser process, a larger mass of argon (4.05 g) is required compared to nitrogen (2.84 g). This difference leads to increased environmental impacts across several categories, such as Ionizing Radiation (+ 14.59%) and Water Consumption (+ 11.46%), with the smallest difference observed in Human Toxicity and Ecotoxicity Indicators.

The Murakami acid and Caro acid treatments within the chemical pre-treatment process are notably impactful, often surpassing the total environmental impact of the entire laser treatment processes across several indicators (Table 9). For instance, in terms of GWP, the Murakami acid process alone contributes with 1.83E−01 kg CO_2 eq, while Caro acid process provides 1.31E−01 kg CO_2 eq which is significantly higher than the total impact of the laser argon pre-treatment, contributing 8.31E−02 kg CO_2 eq, and laser nitrogen pretreatment, 7.81E−02 kg CO_2 eq. Also considering Human Non-Carcinogenic Toxicity, the Caro acid process alone accounts for 2.58E−02 kg 1.4-DCB, whereas the total impact from the laser argon and nitrogen processes are respectively 1.72E−02 kg 1.4-DCB and 1.61E−02 kg 1.4-DCB. The primary responsibility for these impacts lies with potassium ferricyanide in the Murakami acid process, due to its high toxicity and energy-intensive requirements. For the Caro acid process, the critical sub-reagent is hydrogen peroxide, which, combined with waste treatment processes, significantly drives up the environmental impact.

These observations underscore the significant environmental and health burdens imposed by individual chemical processes within the chemical pre-treatment, compared to the overall lower impact of laser-based alternatives. This aligns with findings in the literature, such as those presented by [33, 45], which highlight the lesser environmental impacts of laser treatments relative to chemical processes. These findings confirm the potential of laser-based methods and the imperative to further optimize these processes. Enhancing the longevity of treated substrates could substantially improve the overall sustainability of the diamond coating deposition process.

4.5 Sensitivity Analysis of Pre-treatment Processes

According to ISO 14044, conducting a sensitivity analysis is optional but recommended to verify the robustness and reliability of the obtained results. In this LCA study, the product's service life has emerged as a determining factor for the overall environmental impact. However, to examine variations in results independently of this parameter, a sensitivity analysis has been conducted on the LCA focused solely on pre-treatment processes, using the secondary functional unit and excluding product service life considerations that have been calculated on the basis of a rigorous experimental procedure.

As described in Sect. 3.3, the data used in the LCA inventory come from various sources: some flows were measured directly in the laboratory (primary data), others were obtained from established databases (secondary data), while others were derived from the scientific literature. Among these, the Potassium Ferrocyanide, a sub-reagent used in the modelling of the Murakami acid, and, in particular, the thermal energy required for its synthesis (see Sect. 3.3.1), have proven to be particularly impactful in the environmental results of chemical pre-treatment. A critical aspect of this input data is their obsolescence: the reference sources are outdated [46, 47], and over time, significant technological improvements in production processes may have been implemented. Therefore, to assess the potential effects of such advancements, a one-at-a-time sensitivity analysis, as defined by Groen et al. [66], was conducted. In this analysis, it is assumed that the thermal energy required to synthetize 1 g of Potassium Ferrocyanide has reduced by 10%, 20%, and 30% with respect to the original value of 2.70 MJ (see Table 7). Therefore, three alternative scenarios (ASs) have been defined for this sensitivity analysis: AS1, where the thermal energy is 2.43 MJ (− 10%), AS2, where it is 2.16 MJ (− 20%), and AS3, where it is 1.89 MJ (− 30%).

Table 9 LCIA in terms of characterized ReCiPe Midpoint H for each pre-treatment process, with the split of contributions for each sub-phase

	Pre-treatment chemical (scenario 1.x)						Pre-treatment laser argon (scenario 2.x)				Pre-treatment laser nitrogen (scenario 3.x)			
	Acetone washing	Drying	Murakami acid	Water washing	Caro acid	Water washing	Acetone washing	Drying	Laser argon	Chiller laser	Acetone washing	Drying	Laser nitrogen	Chiller laser
Global warming (kg CO_2 eq)	2.49E−02	2.42E−02	1.83E−01	1.16E−02	1.31E−01	1.16E−02	2.49E−02	2.42E−02	2.64E−02	7.67E−03	2.49E−02	2.42E−02	2.14E−02	7.67E−03
Stratospheric ozone depletion (kg CFC11 eq)	7.90E−09	1.57E−08	4.92E−08	7.71E−09	4.26E−08	7.71E−09	7.90E−09	1.57E−08	1.62E−08	4.98E−09	7.90E−09	1.57E−08	1.38E−08	4.98E−09
Ionizing radiation (kBq Co-60 eq)	1.01E−04	2.06E−04	3.30E−04	9.90E−05	4.21E−04	9.90E−05	1.01E−04	2.06E−04	3.83E−04	6.53E−05	1.01E−04	2.06E−04	2.00E−04	6.53E−05
Ozone formation, Human health (kg NO_x eq)	4.14E−05	4.17E−05	1.32E−04	2.02E−05	1.10E−04	2.02E−05	4.14E−05	4.17E−05	4.59E−05	1.32E−05	4.14E−05	4.17E−05	3.70E−05	1.32E−05
Fine particulate matter formation (kg PM2.5 eq)	2.26E−05	2.75E−05	6.75E−05	1.34E−05	6.47E−05	1.34E−05	2.26E−05	2.75E−05	3.19E−05	8.72E−06	2.26E−05	2.75E−05	2.45E−05	8.72E−06
Ozone formation, Terrestrial ecosystems (kg NO_x eq)	4.46E−05	4.24E−05	1.40E−04	2.06E−05	1.12E−04	2.06E−05	4.46E−05	4.24E−05	4.67E−05	1.35E−05	4.46E−05	4.24E−05	3.77E−05	1.35E−05
Terrestrial acidification (kg SO_2 eq)	6.56E−05	8.07E−05	1.88E−04	3.93E−05	1.49E−04	3.93E−05	6.56E−05	8.07E−05	9.02E−05	2.56E−05	6.56E−05	8.07E−05	7.18E−05	2.56E−05
Freshwater eutrophication (kg P eq)	1.91E−06	9.74E−07	3.21E−06	7.04E−07	6.96E−06	7.04E−07	1.91E−06	9.74E−07	1.47E−06	3.09E−07	1.91E−06	9.74E−07	9.09E−07	3.09E−07
Marine eutrophication (kg N eq)	6.56E−08	6.45E−08	1.06E−06	7.91E−07	1.07E−06	7.91E−07	6.56E−08	6.45E−08	7.93E−08	2.05E−08	6.56E−08	6.45E−08	5.81E−08	2.05E−08

Table 9 (continued)

	Pre-treatment chemical (scenario 1.x)						Pre-treatment laser argon (scenario 2.x)				Pre-treatment laser nitrogen (scenario 3.x)			
	Acetone washing	Drying	Murakami acid	Water washing	Caro acid	Water washing	Acetone washing	Drying	Laser argon	Chiller laser	Acetone washing	Drying	Laser nitrogen	Chiller laser
Terrestrial ecotoxicity (kg 1,4-DCB)	4.27E−02	7.58E−02	1.26E−01	3.69E−02	1.65E−01	3.69E−02	4.27E−02	7.58E−02	7.16E−02	2.41E−02	4.27E−02	7.58E−02	6.60E−02	2.41E−02
Freshwater ecotoxicity (kg 1,4-DCB)	4.28E−05	8.21E−06	1.73E−04	5.49E−06	5.96E−04	5.49E−06	4.28E−05	8.21E−06	8.94E−06	2.61E−06	4.28E−05	8.21E−06	7.29E−06	2.61E−06
Marine ecotoxicity (kg 1,4-DCB)	8.30E−05	5.62E−05	3.49E−04	2.93E−05	9.13E−04	2.93E−05	8.30E−05	5.62E−05	5.62E−05	1.78E−05	8.30E−05	5.62E−05	4.93E−05	1.78E−05
Human carcinogenic toxicity (kg 1,4-DCB)	3.69E−04	3.10E−04	1.10E−03	1.61E−04	3.70E−03	1.61E−04	3.69E−04	3.10E−04	3.13E−04	9.84E−05	3.69E−04	3.10E−04	2.72E−04	9.84E−05
Human non-carcinogenic toxicity (kg 1,4-DCB)	3.79E−03	5.60E−03	1.35E−02	3.03E−03	2.58E−02	3.03E−03	3.79E−03	5.60E−03	6.00E−03	1.78E−03	3.79E−03	5.60E−03	4.95E−03	1.78E−03
Land use (m2a crop eq)	3.12E−04	6.89E−04	1.67E−03	3.33E−04	1.07E−03	3.33E−04	3.12E−04	6.89E−04	7.44E−04	2.19E−04	3.12E−04	6.89E−04	6.10E−04	2.19E−04
Mineral resource scarcity (kg Cu eq)	2.78E−05	4.84E−05	1.37E−04	2.47E−05	1.22E−04	2.47E−05	2.78E−05	4.84E−05	4.90E−05	1.54E−05	2.78E−05	4.84E−05	4.24E−05	1.54E−05
Fossil resource scarcity (kg oil eq)	8.73E−03	7.34E−03	6.06E−02	3.52E−03	1.54E−02	3.52E−03	8.73E−03	7.34E−03	7.83E−03	2.33E−03	8.73E−03	7.34E−03	6.48E−03	2.33E−03
Water consumption (m3)	2.83E−04	4.39E−04	4.42E−04	2.29E−04	7.73E−04	2.29E−04	2.83E−04	4.39E−04	6.86E−04	1.39E−04	2.83E−04	4.39E−04	4.12E−04	1.39E−04

As evidenced by the results of the sensitivity analysis reported in Table 10, the variation in thermal energy required for Potassium Ferrocyanide synthesis influences the environmental impacts of the chemical pre-treatment process. The most sensitive categories include GWP and Fossil Resource Scarcity. Other moderately affected categories are Stratospheric Ozone Depletion, Ozone Formation (both Human Health and Terrestrial Ecosystems), and Terrestrial Acidification. Conversely, Freshwater and Marine Eutrophication and Water Consumption exhibit the smallest reductions, indicating lower sensitivity to thermal energy variations.

Figure 10 illustrates the comparison between the ASs and the laser-based pre-treatment scenarios, highlighting that the gap between chemical pre-treatment and laser pre-treatments remains considerable. Despite the observed impact reductions, achieving the break-even point (i.e. the point where the chemical pre-treatment becomes more sustainable than the laser pre-treatments) would require the complete nullification of the thermal energy usage for all the ReCiPe midpoint categories. This can be considered a non-realistic scenario, even considering the technological advancements and the efficiency improvements of the chemical industry made during the last century. Not even the adoption of alternative energy sources (e.g. solar, wind, waste heat recovery) could lead to a different rank among the three considered pre-treatments. Only a radical change in the chemical process used to synthetize Potassium Ferrocyanide could allow to reach the break-even point.

Summarizing the outcomes, it can be said that despite the outdated nature of the data sourced from the literature that should be improved in further refinement of the present study, the results of the sensitivity analysis confirm the robustness and reliability of the obtained LCA results.

Table 10 Percentage variation of environmental impacts for each ReCiPe midpoint indicator in Alternative Scenarios (ASs) against the baseline pre-treatment chemical

Midpoint indicator	AS1 (%)	AS2 (%)	AS3 (%)
Global warming	−3.85	−7.70	−11.55
Stratospheric ozone depletion	−2.53	−5.06	−7.59
Ionizing radiation	−1.24	−2.48	−3.72
Ozone formation, human health	−2.42	−4.83	−7.25
Fine particulate matter formation	−1.88	−3.76	−5.64
Ozone formation, terrestrial ecosystems	−2.50	−4.99	−7.49
Terrestrial acidification	−2.06	−4.12	−6.18
Freshwater eutrophication	−0.87	−1.74	−2.61
Marine eutrophication	−0.55	−1.10	−1.65
Terrestrial ecotoxicity	−1.09	−2.19	−3.28
Freshwater ecotoxicity	−1.08	−2.16	−3.24
Marine ecotoxicity	−1.32	−2.64	−3.95
Human carcinogenic toxicity	−0.77	−1.53	−2.30
Human non-carcinogenic toxicity	−1.18	−2.36	−3.54
Land use	−1.78	−3.57	−5.35
Mineral resource scarcity	−2.04	−4.08	−6.12
Fossil resource scarcity	−5.40	−10.80	−16.20
Water consumption	−0.37	−0.75	−1.12

5 Conclusions

In conclusion, this study provides a comprehensive evaluation of the environmental impacts associated with diamond coating deposition processes, focusing on a comparison between traditional chemical pre-treatments and innovative laser-based methods.

Considering the sample service life (first functional unit), from the ReCiPe midpoint analysis it emerges that Scenario 1.2 (Chemical Etching with 2% CH_4/H_2) is the least impactful, with the lowest values across most of the indicators (16 on a total of 18). Despite sharing all the processes executed in Scenario 1.1 (Chemical Etching with 1% CH_4/H_2), which ranks as one of the worst, Scenario 1.2 improves the sample's service life by 26.8 times. This improvement can be attributed to the different nanometric cauliflower structure of the diamond coating observed through the SEM images and in accordance with the literature. Scenario 1.2 is also the best according to the GWP analysis, emitting 1.4 kg CO_2 eq, followed by Scenario 3.1 (Laser Argon with 1% CH_4/H_2) with an emission of 1.92 kg CO_2 eq. Even in the ReCiPe endpoint analysis, Scenario 1.2 remains the least impactful, with a total endpoint indicator impact of 4.01E+01 mPt.

By considering the effect of pretreatment alone (second functional unit), the findings reveal that laser pre-treatments generally result in lower environmental impacts than chemical pre-treatments across most ReCiPe midpoint indicators. Water Consumption shows the smallest difference in impact, with laser argon reducing it by 35.4% and laser nitrogen by 46.9% compared to chemical pre-treatment. Conversely, the largest difference is observed in Marine Eutrophication, where laser argons reduce the impact by 94% and laser nitrogen by 94.6% compared to chemical pre-treatment. These findings highlight the potential of laser nitrogen treatments as a more environmentally sustainable alternative to both chemical pre-treatments and laser argon treatments.

A key insight from this analysis is that sample durability, or service life, significantly affects environmental impacts. Improved wear resistance in laser-treated samples, particularly in Scenarios 2.1 and 2.2, leads to lower impacts by minimizing the frequency of

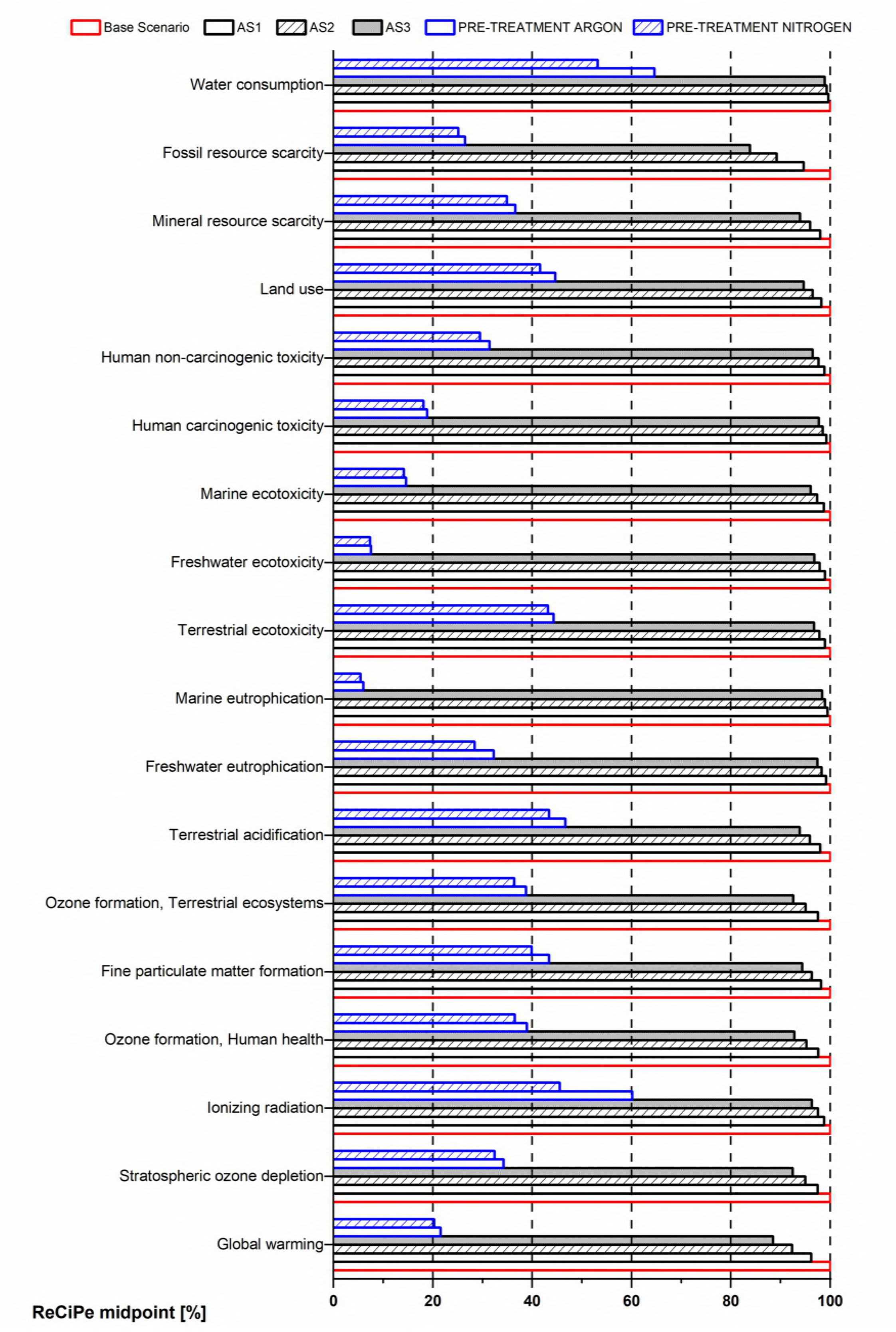

Fig. 10 Detailed comparison among pre-treatment and ASs considering ReCiPe midpoint H indicators (normalization applied)

replacements, thereby lowering cumulative impacts over time. This underscores the need for further technological advancements in laser-based processes to extend the service life of diamond-coated samples. Enhancing the durability of laser-treated samples can be considered an "ecodesign" initiative aimed at minimizing environmental impacts over the lifecycle of the coating. Additionally, improvements to the CVD process are essential, as it remains the most resource-intensive phase of diamond coating. Efficiency enhancements, particularly in the CVD reactor's energy consumption and deposition time, could yield significant environmental benefits. There are different potential optimization strategies which should be explored further for their impact on energy consumption and emissions, such as reducing reactor temperature and deposition duration.

The study's outcomes are subject to certain technological and environmental limitations. First, the data relies on the EcoInvent 3.6 database, which may not capture real-world variability in energy mixes or operational environments. Moreover, specific laboratory conditions and uniform functional units may not fully account for variability in different industrial settings. This limitation could influence the overall reliability of the environmental impact results if scaled to larger production environments.

In addition to technological enhancements, future research should explore environmental and life-cycle cost analyses to provide a broader perspective on the sustainability of diamond coating processes. Life-cycle cost assessments could quantify the economic implications of extending sample service life and optimizing CVD and laser-based treatments, facilitating their feasibility and sustainability.

Appendix

ReCiPe midpoint impact assessment results for the analysed scenarios.

(a) Scenario 1.1

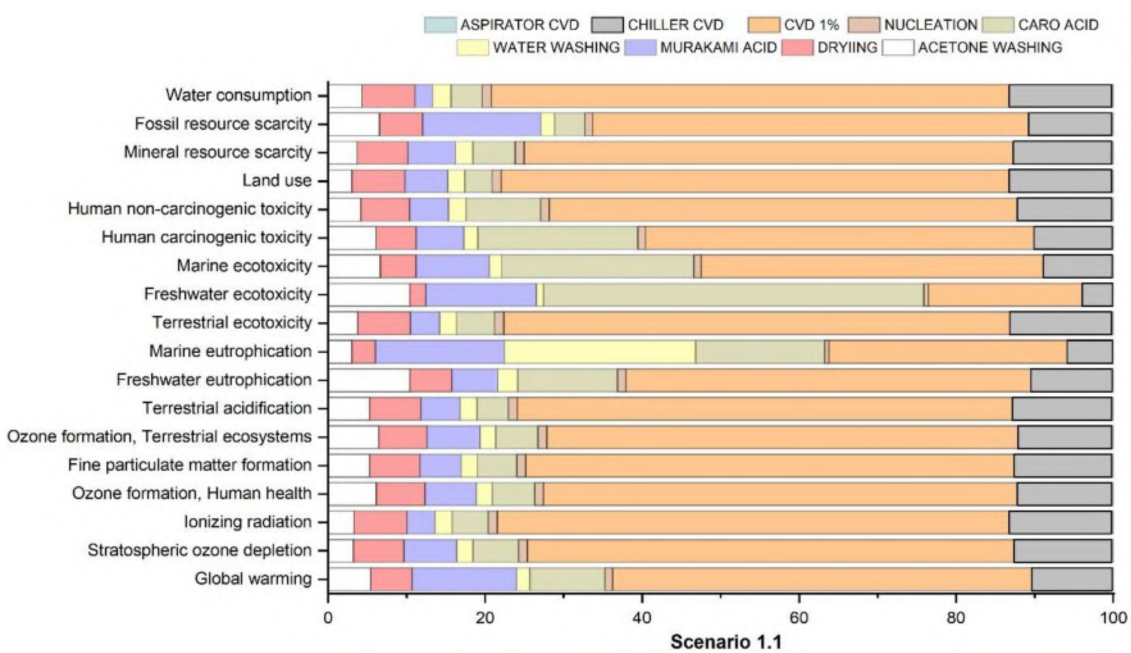

(b) Scenario 1.2

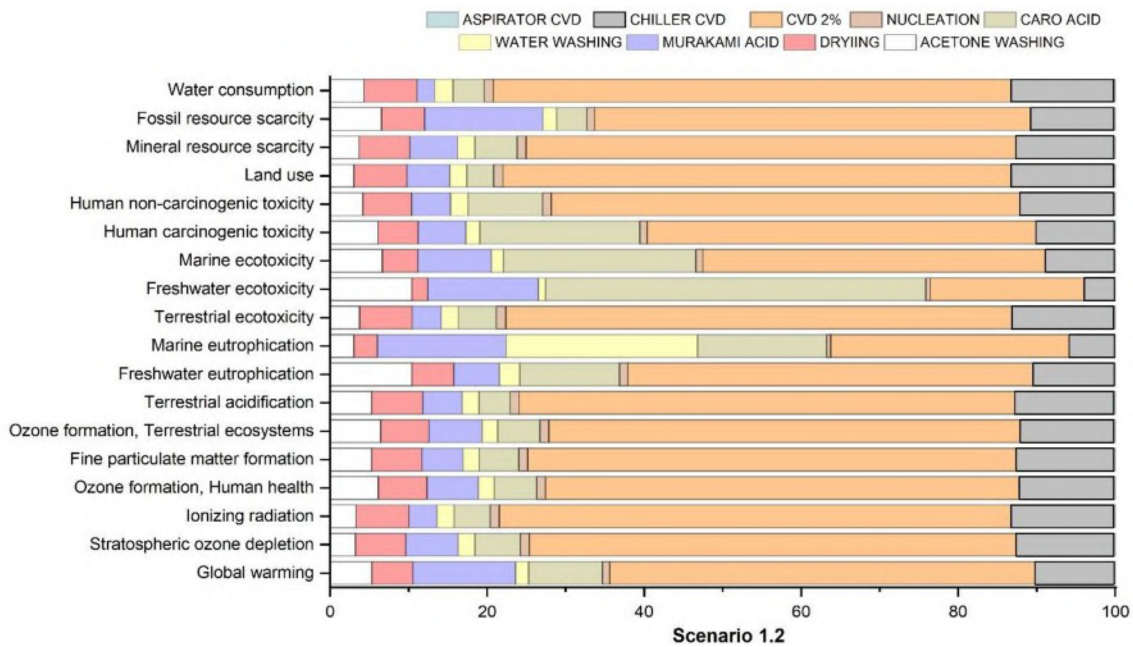

(c) Scenario 2.1

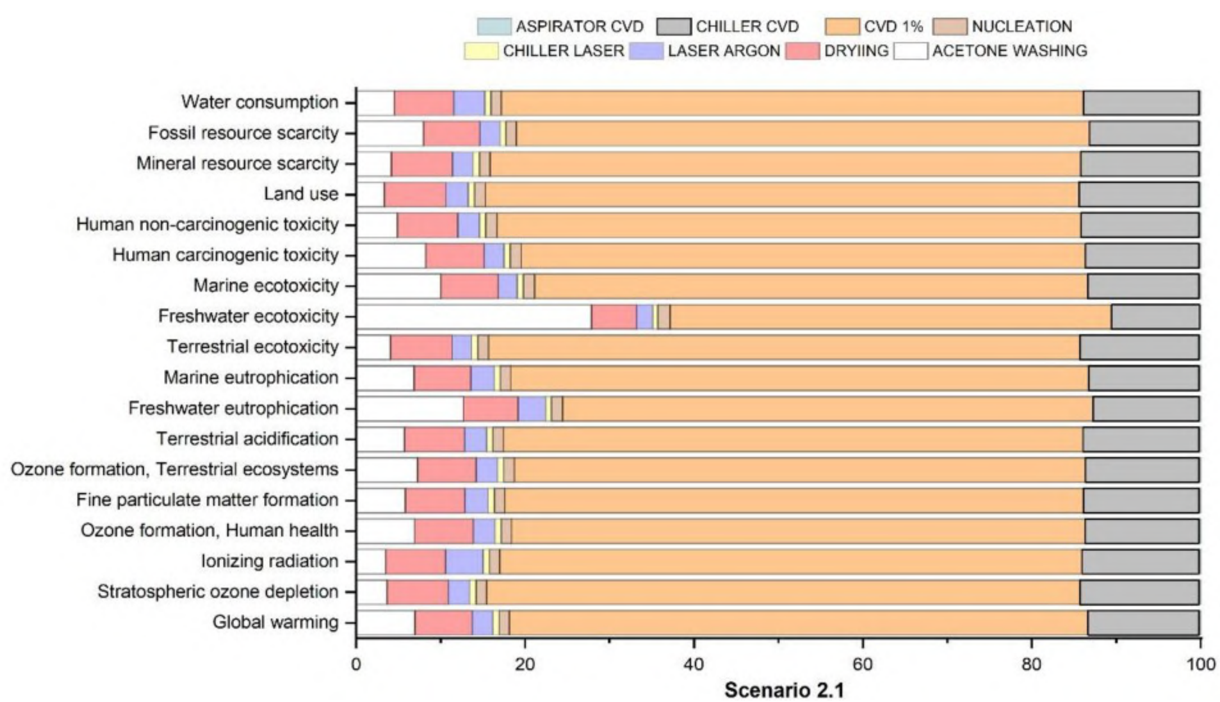

(d) Scenario 2.2

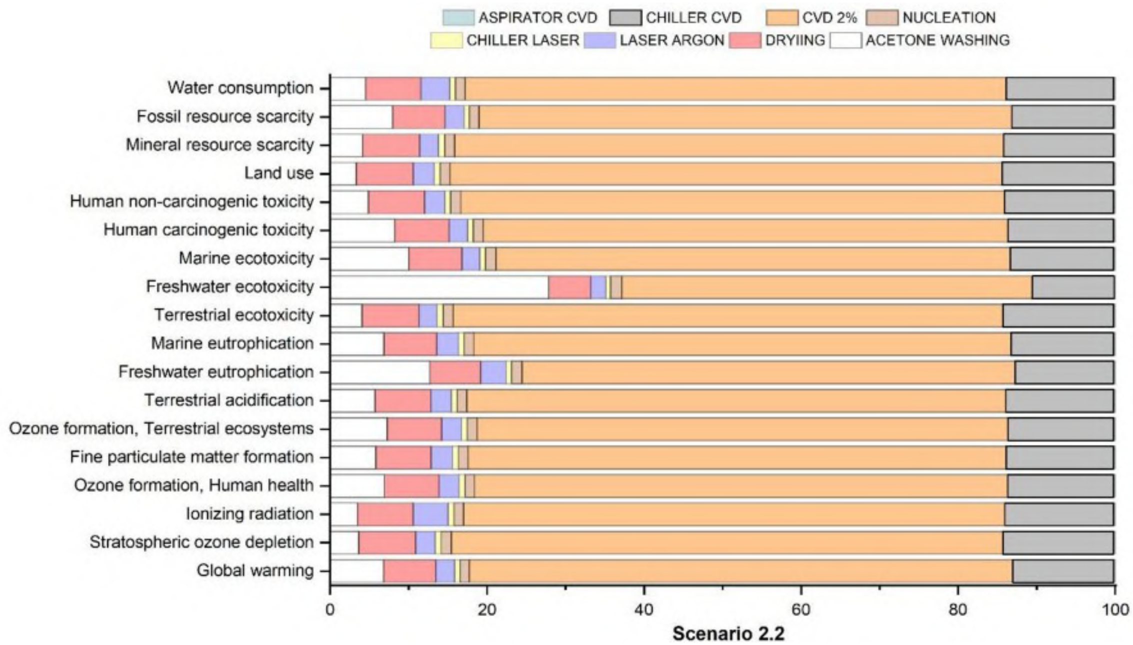

(e) Scenario 3.1

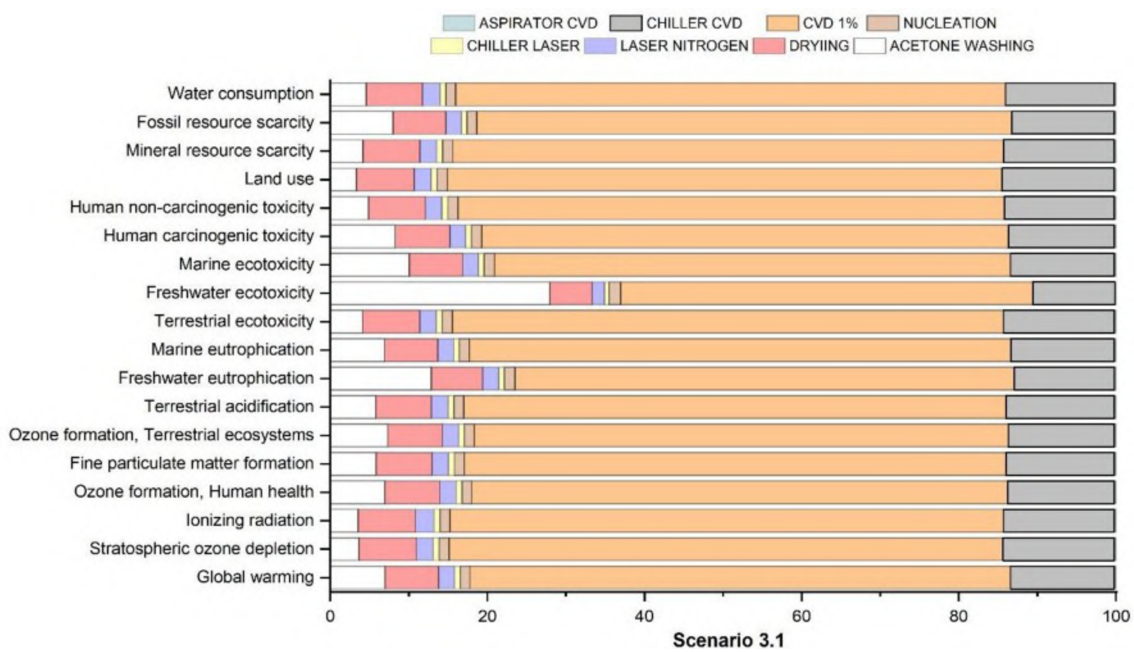

(f) Scenario 3.2

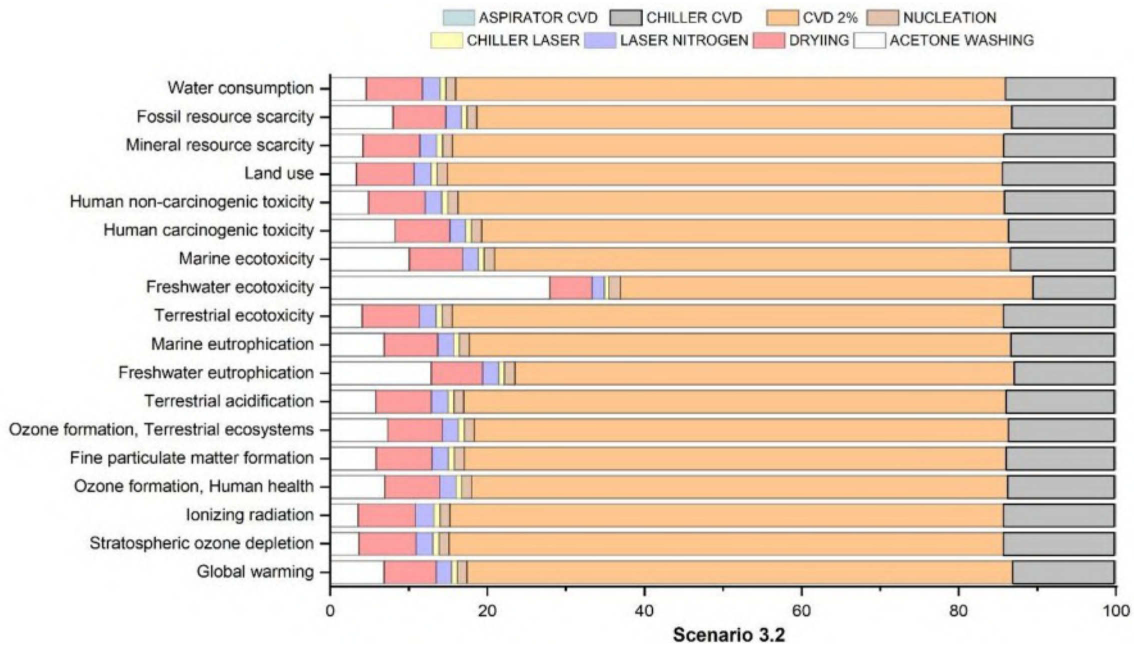

Declarations

Conflict of interest The authors declare that they have no known competing financial interests or personal relationships that could have appeared to influence the work reported in this paper.

References

1. Schalk, N., Tkadletz, M., & Mitterer, C. (2022). Hard coatings for cutting applications: Physical vs. chemical vapor deposition and future challenges for the coatings community. *Surface and Coatings Technology, 429*, 127949. https://doi.org/10.1016/j.surfcoat.2021.127949
2. Guo, Z., Guo, B., Zhang, J., et al. (2024). CVD diamond processing tools: A review. *Journal of Advanced Research*. https://doi.org/10.1016/j.jare.2024.09.013
3. Ma, Y. P., Sun, F. H., Xue, H. G., et al. (2007). Deposition and characterization of nanocrystalline diamond films on Co-cemented tungsten carbide inserts. *Diamond and Related Materials, 16*, 481–485. https://doi.org/10.1016/j.diamond.2006.09.020
4. Lee, Y. J., & Wang, H. (2024). Sustainability of Methods for Augmented Ultra-Precision Machining. *International Journal of Precision Engineering and Manufacturing-Green Technology, 11*, 585–624. https://doi.org/10.1007/s40684-023-00546-z
5. Hakovirta, M. (1996). Adhesion of amorphous diamond-like film on sputtered hardmetal (WC-Co) cutting tools. *Diamond and Related Materials, 5*, 186–189. https://doi.org/10.1016/0925-9635(95)00497-1
6. Sedov, V., Martyanov, A., Ashkinazi, E., et al. (2023). Effect of diamond seeds size on the adhesion of CVD diamond coatings on WC-Co instrument. *Surfaces and Interfaces, 38*, 102861. https://doi.org/10.1016/j.surfin.2023.102861
7. Polini, R., Bravi, F., Mattei, G., et al. (2002). Effect of WC grain growth inhibitors on the adhesion of chemical vapor deposition diamond films on WC–Co cemented carbide. *Diamond and Related Materials, 11*, 242–248. https://doi.org/10.1016/S0925-9635(01)00681-1
8. Wang, X., & Ye, J. (2024). Interface characteristics of CVD diamond coating on WC-Co cemented carbide substrate. *Surface and Coatings Technology, 485*, 130886. https://doi.org/10.1016/j.surfcoat.2024.130886
9. Baek, S. Y., Park, J., Koh, T., et al. (2024). Achievement of green and sustainable CVD through process, equipment and systematic optimization in semiconductor fabrication. *International Journal of Precision Engineering and Manufacturing-Green Technology, 11*, 1295–1316. https://doi.org/10.1007/s40684-024-00606-y
10. Xu, F., Xu, J. H., Yuen, M. F., et al. (2013). Adhesion improvement of diamond coatings on cemented carbide with high cobalt content using PVD interlayer. *Diamond and Related Materials, 34*, 70–75. https://doi.org/10.1016/j.diamond.2013.01.012
11. Chandran, M. (2022). Diamond deposition on WC–Co substrates with interlayers for engineering applications. In *Nanomaterials for sensing and optoelectronic applications* (pp. 311–330). Elsevier
12. Truscott, B. S., Kelly, M. W., Potter, K. J., et al. (2016). Microwave plasma-activated chemical vapor deposition of nitrogen-doped diamond. II: $CH_4/N_2/H_2$ plasmas. *Journal of Physical Chemistry A, 120*, 8537–8549. https://doi.org/10.1021/acs.jpca.6b09009
13. Tzeng, Y., Chen, W. L., Wu, C., et al. (2013). The synthesis of graphene nanowalls on a diamond film on a silicon substrate by

direct-current plasma chemical vapor deposition. *Carbon N Y, 53*, 120–129. https://doi.org/10.1016/j.carbon.2012.10.038
14. Chen, X., & Narayan, J. (1993). Effect of the chemical nature of transition-metal substrates on chemical-vapor deposition of diamond. *Journal of Applied Physics, 74*, 4168–4173. https://doi.org/10.1063/1.354420
15. Cappelli, E., Pinzari, F., Ascarelli, P., & Righini, G. (1996). Diamond nucleation and growth on different cutting tool materials: Influence of substrate pre-treatments. *Diamond and Related Materials, 5*, 292–298. https://doi.org/10.1016/0925-9635(95)00426-2
16. Polini, R. (2006). Chemically vapour deposited diamond coatings on cemented tungsten carbides: Substrate pretreatments, adhesion and cutting performance. *Thin Solid Films, 515*, 4–13. https://doi.org/10.1016/j.tsf.2005.12.042
17. Da Silva Neto, J. V., Rodríguez, L. A. A., Fraga, M. A., et al. (2016). WC-Co substrate preparation and deposition conditions for high adhesion of CVD diamond coating. *Revista Brasileira de Aplicações de Vácuo, 35*, 53. https://doi.org/10.17563/rbav.v35i1.1015
18. Tang, Y., Li, Y. S., Yang, Q., & Hirose, A. (2010). Deposition and characterization of diamond coatings on WC-Co cutting tools with W/Al interlayer. *Diamond and Related Materials, 19*, 496–499. https://doi.org/10.1016/j.diamond.2009.12.019
19. Ye, F., Li, Y., Sun, X., et al. (2016). CVD diamond coating on WC-Co substrate with Al-based interlayer. *Surface and Coatings Technology, 308*, 121–127. https://doi.org/10.1016/j.surfcoat.2016.06.088
20. Barletta, M., Rubino, G., & Gisario, A. (2011). Adhesion and wear resistance of CVD diamond coatings on laser treated WC–Co substrates. *Wear, 271*, 2016–2024. https://doi.org/10.1016/j.wear.2011.01.042
21. Barletta, M., Rubino, G., Valle, R., & Polini, R. (2012). Chemical vapor deposition of highly adherent diamond coatings onto Co-cemented tungsten carbides irradiated by high power diode laser. *ACS Applied Materials and Interfaces, 4*, 694–701. https://doi.org/10.1021/am2012992
22. Vidal, R., Alberola-Borràs, J.-A., Gómez-Cordón, J., et al. (2017). LCA to evaluate the environmental impact for chemical pre-treatment in plastics metallization. *Journal of Polymers and the Environment, 25*, 961–972. https://doi.org/10.1007/s10924-016-0872-6
23. Johnson, A. D., Ridgeway, R. G., & Maroulis, P. J. (2004). Reduction of PFC emissions to the environment through advances in CVD and etch processes. *IEEE Transactions on Semiconductor Manufacturing, 17*, 491–496. https://doi.org/10.1109/TSM.2004.835700
24. Nesladek, M., Spinnewyn, J., Asinari, C., et al. (1994). Improved adhesion of CVD diamond films to steel and WC-Co substrates. *Diamond and Related Materials, 3*, 98–104. https://doi.org/10.1016/0925-9635(94)90038-8
25. Wang, X., Shen, X., Gao, J., & Sun, F. (2017). Consecutive deposition of amorphous SiO_2 interlayer and diamond film on graphite by chemical vapor deposition. *Carbon N Y, 117*, 126–136. https://doi.org/10.1016/j.carbon.2017.02.051
26. Kaushal, I., & Chakrabarti, A. (2023). System modelling for collecting life cycle inventory (LCI) data in MSMEs using a conceptual model for smart manufacturing systems (SMSs). *International Journal of Precision Engineering and Manufacturing-Green Technology, 10*, 819–834. https://doi.org/10.1007/s40684-022-00489-x
27. Venettacci, S., Ponticelli, G. S., & Guarino, S. (2021). Fluidised bed finishing process for aeronautical applications: Environmental and technical-economic assessment. *Journal of Cleaner Production, 299*, 126900. https://doi.org/10.1016/j.jclepro.2021.126900
28. Carneiro, J. L., Rodriguez, C., Figueiredo, M. C., & Freire, F. (2024). Ex-ante life cycle assessment of emerging and novel technologies. *Encyclopedia of Sustainable Technologies, 1*, 194–212. https://doi.org/10.1016/B978-0-323-90386-8.00092-9
29. Gonzales, J. S., Rumaior, M., Ramos, A. D., Irabien, A., & Ortiz, I. (2023). The relevance of life cycle assessment tools in the development of emerging decarbonization technologies. *JACS Au, American Chemical Society, 3*(10), 2631–2639. https://doi.org/10.1021/jacsau.3c00276
30. Xiong, Y., Lau, K., Zhou, X., & Schoenung, J. M. (2008). A streamlined life cycle assessment on the fabrication of WC–Co cermets. *Journal of Cleaner Production, 16*, 1118–1126. https://doi.org/10.1016/j.jclepro.2007.05.007
31. Bianco, I., & Blengini, G. A. (2019). Life Cycle Inventory of technologies for stone quarrying, cutting and finishing: Contribution to fill data gaps. *Journal of Cleaner Production, 231*, 419–427. https://doi.org/10.1016/j.jclepro.2019.05.170
32. Wilfong, C., Gomez, H., Durham, D. (2012). Life cycle analysis of diamond coating of machining tools. In *ASME 2012 International manufacturing science and engineering conference* (pp. 1049–1056). American Society of Mechanical Engineers.
33. Marconi, M., Pietroni, G., & Rubino, G. (2022). Comparing the environmental and economic performances of different substrate pre-treatment processes for diamond coating deposition. *Procedia CIRP, 105*, 476–481. https://doi.org/10.1016/j.procir.2022.02.079
34. ISO-International Organization for Standardization. (2015). ISO EN 14001, Environmental management systems—requirements with guidance for use.
35. Barletta, M., Rubino, G., & Gisario, A. (2011). Co removal and phase transformations during high power diode laser irradiation of cemented carbide. *Applied Surface Science, 257*, 4239–4245. https://doi.org/10.1016/j.apsusc.2010.12.027
36. Straffelini, G., Scardi, P., Molinari, A., & Polini, R. (2002). Erratum to "Characterization and sliding behavior of HFCVD diamond coatings on WC–Co." *Wear, 252*, 1020. https://doi.org/10.1016/S0043-1648(02)00041-8
37. Polini, R., Barletta, M., Rubino, G., & Vesco, S. (2012). Recent advances in the deposition of diamond coatings on Co-cemented tungsten carbides. *Advances in Materials Science and Engineering, 2012*, 1–14. https://doi.org/10.1155/2012/151629
38. Prieske, M., Müller, S., & Woizeschke, P. (2019). Interaction of methane concentration and deposition temperature in atmospheric laser based CVD diamond deposition on hard metal. *Coatings, 9*(9), 537. https://doi.org/10.3390/coatings9090537
39. Tankala, K., & DebRoy, T. (1992). Modeling of the role of atomic hydrogen in heat transfer during hot filament assisted deposition of diamond. *Journal of Applied Physics, 72*(2), 712–718. https://doi.org/10.1063/1.351857
40. Polini, R., Barletta, M., & Cristofanilli, G. (2010). Wear resistance of nano- and micro-crystalline diamond coatings onto WC–Co with Cr/CrN interlayers. *Thin Solid Films, 519*, 1629–1635. https://doi.org/10.1016/j.tsf.2010.07.128
41. May, P. W., Ludlow, W. J., Hannaway, M., et al. (2008). Raman and conductivity studies of boron-doped microcrystalline diamond, facetted nanocrystalline diamond and cauliflower diamond films. *Diamond and Related Materials, 17*, 105–117. https://doi.org/10.1016/j.diamond.2007.11.005
42. Williams, O. A., Daenen, M., D'Haen, J., et al. (2006). Comparison of the growth and properties of ultrananocrystalline diamond and nanocrystalline diamond. *Diamond and Related*

Materials, 15, 654–658. https://doi.org/10.1016/j.diamond.2005.12.009

43. ISO-International Organization for Standardization. (2006). ISO EN 14040, environmental management—life cycle assessment—principles and framework.
44. ISO-International Organization for Standardization. (2006). ISO EN 14044, environmental management—life cycle assessment—requirements and guidelines.
45. Favi, C., Marconi, M., Mandolini, M., & Germani, M. (2022). Sustainable life cycle and energy management of discrete manufacturing plants in the industry 40 framework. *Applied Energy, 312*, 118671. https://doi.org/10.1016/j.apenergy.2022.118671
46. Barsky, G. (1926). Method of making potassium ferricyanide. U.S. Patent No. 60,046.
47. Buchanan, G. H., & Hulings, C. M. (1928). Process of producing potassium ferrocyanide. U.S. Patent No. 702,424.
48. Werle P. TM, DU. (1993). Process for the production of calcium formate.
49. Forcellese, A., Marconi, M., Simoncini, M., & Vita, A. (2020). Life cycle impact assessment of different manufacturing technologies for automotive CFRP components. *Journal of Cleaner Production, 271*, 122677. https://doi.org/10.1016/j.jclepro.2020.122677
50. Goedkoop, M., Heijungs, R., Huijbregts, M., De Schryver, A., Struijs, J., van Zelm, R. (2009). ReCiPe 2008: a life cycle impact assessment method which comprises harmonised category indicators at the midpoint and the endpoint level. In *Report I: Character*.
51. Furberg, A., & Arvidsson, R. (2024). Life cycle assessment of synthetic nanodiamond and diamond film production. *ACS Sustain Chem Eng, 12*, 365–374. https://doi.org/10.1021/acssuschemeng.3c05854
52. Verbitsky, O., & Pushkar, S. (2018). Eco-indicator 99, ReCiPe and ANOVA for evaluating building technologies under LCA uncertainties. *Environmental Engineering and Management Journal, 17*, 2549–2559. https://doi.org/10.30638/eemj.2018.253
53. Alyaseri, I., & Zhou, J. (2017). Towards better environmental performance of wastewater sludge treatment using endpoint approach in LCA methodology. *Heliyon, 3*, e00268. https://doi.org/10.1016/j.heliyon.2017.e00268
54. Efthymiou, M., & Papatheodorou, A. (2019). EU emissions trading scheme in aviation: Policy analysis and suggestions. *Journal of Cleaner Production, 237*, 117734. https://doi.org/10.1016/j.jclepro.2019.117734
55. Stocker, T. F., Qin, D., Plattner, G.-K., Tignor, M. M. B., Allen, S. K., Boschung, J., Nauels, A., Xia, Y., Bex, V., & Midgley, P. M. (2013). IPCC Climate Change 2013: The physical science basis. Working Group I contribution to the fifth assessment report.
56. Liu, Y., Zhao, Z., Wang, Q., et al. (2024). Insights into the removal of volatile organic compounds by three-dimensional ordered microporous zeolite-templated carbon: A combined experimental study and density functional theory calculation. *Chemical Engineering Journal, 494*, 152965. https://doi.org/10.1016/j.cej.2024.152965
57. Kopec, M. (2024). Recent advances in the deposition of aluminide coatings on nickel-based superalloys: A synthetic review (2019–2023). *Coatings, 14*, 630. https://doi.org/10.3390/coatings14050630
58. Jing, X., Lv, C., Zhang, H., et al. (2024). One-step fabrication of P-Co5.47N/Co9S8@NPC heterojunction derived from saccharomycetes cerevisiae as environment-friendly bifunctional high-efficiency electrocatalysts. *Colloids and Surfaces A: Physicochemical and Engineering Aspects, 697*, 134411. https://doi.org/10.1016/j.colsurfa.2024.134411
59. Garg, R., & Singh, S. K. (2023). Sources and toxicity assessment of cyanide from iron and steel industry wastewater (pp. 183–189).
60. Shi, P., Yue, X., Teng, X., et al. (2024). Degradation of butylated hydroxyanisole by the combined use of peroxymonosulfate and ferrate(VI): Reaction kinetics, mechanism and toxicity evaluation. *Toxics, 12*, 54. https://doi.org/10.3390/toxics12010054
61. Montes, L., Rico, V., Nuñez-Galvez, F., et al. (2024). Long-lasting low fluorinated stainless steel hierarchical surfaces for omniphobic, anti-fouling and anti-icing applications. *Surfaces and Interfaces, 46*, 104167. https://doi.org/10.1016/j.surfin.2024.104167
62. Health Effects Institute. (2023). Health effects of air pollution. State of global air. https://www.stateofglobalair.org/health/pm
63. Sharma, S., Chandra, M., & Kota, S. H. (2020). Health effects associated with PM2.5: A systematic review. *Curr Pollut Rep, 6*, 345–367. https://doi.org/10.1007/s40726-020-00155-3
64. European Chemicals Agency. (2023). Substance information: Potassium peroxymonosulfate triple salt. ECHA. https://echa.europa.eu/it/substance-information/-/substanceinfo/100.033.916
65. McMichael, T., Montgomery, H., & Costello, A. (2012). Health risks, present and future, from global climate change. *BMJ, 344*, e1359–e1359. https://doi.org/10.1136/bmj.e1359
66. Groen, E., Heijungs, R., Bokkers, E. A. M., & Boer, I. J. M. (2014). Sensitivity analysis in life cycle assessment. In *Proceedings of the 9th international conference on life cycle assessment in the agri-food sector* (LCA food 2014) (pp. 482–488). https://edepot.wur.nl/331109

Dr. Emanuele Mingione Ph.D., is a researcher in the disciplinary scientific sector - Processing Technologies and Systems - at the Department of Economics, Engineering, Society and Business Organization, University of Tuscia, Viterbo (VT). He received his M.S. degree in Mechanical Engineering with honors in 2018 and his Ph.D. degree in Engineering for Industrial Design and Production in 2022 from the Department of Business Engineering, University of Rome Tor Vergata, Rome (RM). He actively collaborates with the Tor Vergata University research group on issues related to the implementation of innovative engineering materials for 3D printing and innovative Manufacturing processes.

Dr. Mattia Gianvincenzi Ph.D., is a research fellow in Engineering for Energy and Environment and serves as an Adjunct Professor in the Master's program on Management Innovation for Competitive Finance and European Project Planning at the University of Tuscia. His research focuses on battery sustainability, Life Cycle Assessment, European regulations, data traceability, digitalization, and eco-design. With extensive expertise in designing and managing European funding projects, he has collaborated with international academic institutions and companies on innovation and sustainability initiatives.

Prof. Marco Marconi Ph.D., is Associate Professor in Design methods for industrial engineering at theUniversità degli Studi della Tuscia, Viterbo, Italy. His reaserch interests mainly regards: Methods and tools for sustainable design, with a focus on the development of design supporting methods and software tools based on the concept of life cycle thinking and assessment and on a preventive and goal-oriented approach; Digital & Sustainable manufacturing, with a focus on methods and tools to facilitate the digital and sustainable transition of industrial processes through the implementation of Industry 4.0 and 5.0 technologies and advanced data processing techniques.

Prof. Gianluca Rubino Ph.D., is Associate Professor in ING-IND/16 - Processing Technologies and Systems at the Department of Economics, Engineering, Society and Business Organization, University of Tuscia, Viterbo, Italy. He received his MS degree in Mechanical Engineering in 2005 and his PhD in Industrial Engineering materials engineering curriculum in 2009 from the Department of Industrial Engineering, University of Rome Tor Vergata, Italy. Rubino's scientific activity is entirely focused on topics related to Processing Technologies and Systems, dealing mainly with the development and implementation of innovative engineered materials and on related manufacturing technologies.